Department of Pathobiology
University of Veterinary Medicine Vienna
Institute of Immunology
(Head: Univ.-Prof. Dr. rer. nat. A. Saalmüller)

SOLVING TECHNICAL ISSUES TO CHARACTERIZE PORCINE CD8alpha/beta EXPRESSING LYMPHOCYTES

BACHELOR THESIS

for obtaining the degree

Bachelor of Science (B.Sc.)

of the University of Veterinary Medicine Vienna

submitted by

Florian Ringl

Vienna, June 2023

Supervisor: Kerstin Mair, PhD.

Reviewer: Mag. Dr. Silivio Kau, MSc.

Acknowledgement

First, I would like to thank Armin Saalmüller for giving me the opportunity to write my bachelor thesis at the Institute of Immunology of the University of Veterinary Medicine Vienna. I would like to thank the entire team, especially Maria and Katinka who supported me with the practical work in the laboratory.

In particular, I would like to thank my supervisor Kerstin Mair who was always there for me during the work, for her patience and for her enormous expertise, which helped me to better understand certain topics in immunology. I am very grateful that you were always open to questions and that you offered me my first insights into writing a scientific thesis!

Finally, I would like to express my gratitude to my parents who made it possible for me to study "Biomedicine and Biotechnology ". I also would like to thank them for their financial support throughout my entire time as a student!

Table of contents

Abbreviations

APCs	Antigen Presenting Cells
CD	Cluster of Differentiation
CDR	Complementary Determining Region
CTL	Cytolytic T-Lymphocytes
DMSO	Dimethyl Sulfoxide
Fab	Antigen Binding Fragment
Fc	Constant Fragment
FCM	Flow Cytometry
FCS	Fetal Calf Serum
FSC	Forwards Scatter
INF	Interferon
Ig	Immunoglobulin
IL	Interleukin
LSM	Lymphocyte Separation Medium
mAbs	Monoclonal Antibodies
MHC	Major Histocompatibility Complex
NK-cells	Natural Killer Cells
PAMP	Pathogen Associated Molecular Patterns
PBL	Peripheral Blood Lymphocytes
PBMC	Peripheral Blood Mononuclear Cells
PBS	Phosphate Buffered Saline
PE	Phycoerythrin
PE-Cy7	Phycoerythrin-Cyanine7
PRR	Pathogen Recognition Receptors
RT	Room Temperature
SH	Steric Hindrance
SOP	Standard Operating Procedure
SSC	Sidewards Scatter
TCR	T-Cell Receptor

Th-cells	T-Helper Cells
TNF	Tumour Necrosis Factor

1 Introduction

1.1 The Role of the pig in immunological research

Within biomedical research, the domestic pig (*Sus scrofa domesticus*) is a very good animal to study human diseases of any kind. This is due to the numerous similarities with humans in terms of anatomy and physiology (Käser 2021; Pabst 2020; Gerdts et al. 2015). For example, the porcine immune system resembles over 80 % of the human immune system, while that of mice only about 10 % (Dawson 2011). In addition, there are numerous markers with which immune cells and their specific development and behaviour in the lymphatic organs can be studied. The pig is currently the best researched model for possible future xenotransplantation to alleviate the problem of organ shortage in organ transplants (Pabst 2020). All in all, the pig offers many advantages compared to other animal species used in research such as mice, dogs or monkeys (Pabst 2020). A good general understanding about the porcine immune system is therefore an important prerequisite for the study of immunological diseases. Furthermore, it is important to study the porcine immune system in more detail for improving animal welfare in this farm animal species.

1.2 Immune system of mammals in general - with focus on the pig

The immune system is the defence system of biological organisms. It can distinguish between foreign and endogenous substances and thus offers protection against pathogens of any kind. The classification of the immune system and the associated immune reaction is based on several factors. The most important aspect is the division into a less-specific (innate) and a specific (acquired or adaptive) immune system, as well as the distinction between cellular and non cellular (humoral) immune defence (McComb et al. 2019).

The immune system forms a specialized network of immune organs that cooperate with each other. Due to the lymph and blood vessels, it is possible for the immune system to supply several areas in the organism simultaneously. The primary lymphoid organs are the tissues responsible to produce lymphoid cells from precursor cells, these include the bone marrow and the thymus. The antigen presentation and the clonal proliferation of the lymphocytes take place in the secondary lymphoid organs (spleen, lymph nodes, Peyer’s patches, appendix and mucosa associated lymphoid tissue) (McComb et al. 2019).

The response of the innate system is characterized primarily by a rapid response that is less specific for distinct pathogens (Saalmüller 2006).The cells of the porcine innate immune system generally include granulocytes, mast cells, macrophages, dendritic cells, and lymphocytes like γδ T cells and natural killer (NK) cells (Mair et al. 2014). Humoral components include the complement system, which is composed of several soluble plasma proteins, acute phase proteins and antimicrobial peptides (Shishido et al. 2012).

Like for other mammalian species, the first step in the innate immune response of the pig includes pathogen recognition by antigen presenting cells (APCs, macrophages and dendritic cells). Highly conserved pathogen associated molecular patterns (PAMPs) such as lipopolysaccharides are recognized with the help of pathogen recognition receptors (PRRs) (Kumar and Kawai 2011). APCs can ingest (phagocytose) the pathogens and subsequently release pro-inflammatory chemokines and cytokines (e.g., Interleukin (IL)-8, IL-1β, IL 6, IL 12, or tumour necrosis factor α (TNF-α) (Saalmüller 2006). Together with the complement system, acute phase proteins and antimicrobial peptides, these immunological messengers are part of the first defence (Mair et al. 2014).

After phagocytosis, the antigen-presenting cells process and present peptide-fragments (antigens) of the pathogens on their surface to the B and T lymphocytes, thus activating the adaptive arm of the immune system. Antigen-specific lymphocytes are then activated and can kill the pathogens directly, provide B-cell help (T cells), or produce antibodies which mark and neutralize the pathogens (B cells). In addition, memory cells are produced, which form the basis for immunological memory important for a second encounter with the pathogen (McComb et al. 2019). The reaction of the adaptive immune system is characterized by antigen specificity slower but more specific immune responses and the development of a long-lasting immunological memory (Saalmüller 2006). In the following chapters, certain lymphocyte populations within the innate and adaptive immune system are discussed in more detail, especially the role of T lymphocytes and highlighting the role of the CD8 cell-surface molecule.

1.3 The CD8 receptor

The CD8 molecule is a surface glycoprotein, that plays an essential role in the immune system of higher organism. The receptor consists of two amino acid chains, which are held together by disulfide bonds. For interaction with the major histocompatibility complex (MHC), the

polypeptide chains possess a single immunoglobulin like domain on the extracellular side of the receptor. The chains are anchored in the membrane with the help of other polypeptides. The CD8 receptor is expressed in two different isoforms. Typically, it is represented in the form of an αβ heterodimer, consisting of an α and a β chain. The other variant is the expression of an αα homodimer consisting of two identical α chains (Terry et al. 1990; Saalmüller et al. 1994). The monomer structure has a molecular weight of 33-35 kDa, while the dimer has a molecular weight of 66-70 kDa (Jonjić and Koszinowski 1984; Pescovitz et al. 1984). CD8 serves as a coreceptor of the T-cell receptor (TCR). The TCR recognizes the epitope presented on MHC-class-I molecules and CD8 interacts with the associated α3 domain of the MHC-class-I complex (Figure 1) (Devine et al. 1999).

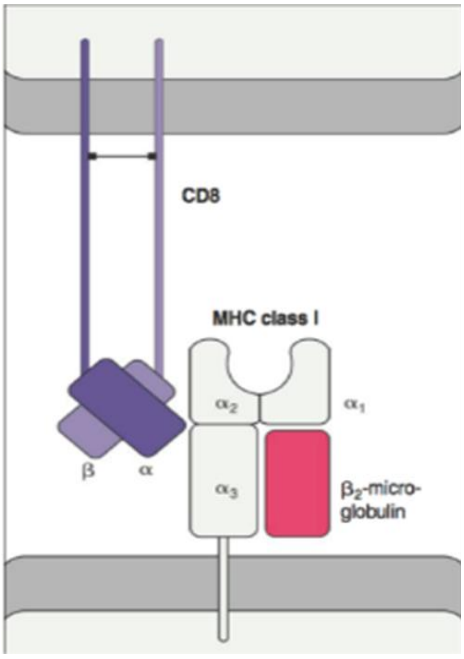

Figure 1: Interaction between CD8 heterodimer and MHC-class-I
The figure shows the interaction of the CD8 receptor (consisting of an α and a β chain) and the α3 domain of the MHC class one molecule.
From: Janeway's Immunobiology 8th edition GS

The CD8 receptor is expressed by several lymphocyte subsets in the pig, including NK cells, γδ T cells and antigen-experienced αβ T cells. On these cell populations, CD8 is expressed as an α homodimer. Porcine cytolytic T cells on the other hand exclusively express CD8 αβ heterodimers (Gerner et al. 2009). Several monoclonal antibodies (mAbs) for either of the two

chains are available. Certain mAb clones are known that can recognize different epitopes only in the CD8α chain (epitope CD8a and CD8b) (Saalmüller et al. 1994). Nonetheless, no detailed information is available on the distinct epitopes of the mAbs.

1.4 Porcine T lymphocytes and their development

As in other higher mammals, the thymus of swine is an organ responsible for the maturation and production of T cells. From day 40 of gestation, the thymus is colonized by precursor thymocytes. These progenitor cells are produced in the liver during the first fetal trimester and do not yet express cluster of differentiation (CD) surface molecules CD3, CD4, or CD8 (referred to as double-negative thymocytes). After 40-50 days of gestation, they begin to express CD3, but unlike murine or human double-negative thymocytes, porcine double-negative thymocytes do not express the CD25 molecules (Sinkora et al. 2000; Sinkora and Butler 2009). In general, most double-negative thymocytes express the γδ T-cell receptor. The γδ TCR population dominates the thymus and peripheral lymphoid tissue (e.g., spleen) between 40-60 days of fetal life. Double-negative thymocytes, which do not express the γδ TCR, begin to express both CD4 and CD8 at approximately 60-70 days post gestation. These cells are called double-positive thymocytes and become the predominant population after 60-90 days of gestation. At day 70, they differentiate to either $CD4^+CD8^-$ or $CD4^-CD8^+$. As in humans porcine T cell progenitors that enter the thymus during and after the third trimester of gestation originate from the bone marrow and no longer from the liver (Sinkora et al. 2000; Gerner et al. 2009).

Regarding human and mouse thymocytes, it is well reported that only those developing T cells expressing their specific T-cell receptor molecules, capable of recognizing the self-major histocompatibility complex (MHC) antigen molecules, but not endogenous antigens differentiate into specific mature non-self-reactive lymphocytes, while cells with reactivity against their own organism are eliminated by apoptosis (Anderson et al. 1996). To date, little is known about positive and negative selection of T cells in pigs (Charerntantanakul and Roth 2006). It is assumed that the selection of T cells in pigs takes place in the second and third trimesters of gestation, since a particularly large number of thymocytes die at this period (Sinkora et al. 1998). The positive selection leads to T cells subsequently recognizing foreign substances, only if their antigens are bound to the MHC on the surface of other cells. Free antigens are only recognized by T cells if they are actively presented by antigen presenting cells

(so called MHC restriction). However, porcine γδ T cells can recognize antigens independently and without the help of the MHC (Charerntantanakul and Roth 2006; Takamatsu et al. 2006).

1.4.1 Classification and characterization of porcine T cells

1.4.2 T-cell receptor and clusters of differentiation (CD)

Porcine T cells are divided into various subgroups with characteristic features and functions. The T cells are phenotypically classified by a different structure of the TCR and additionally based on specific surface coreceptors. All T cells are defined by the expression of the CD3 molecule (Saalmüller et al. 1999; Charerntantanakul and Roth 2006). Regarding the structure of the TCR, a distinction is made between two main forms. The αβ T cells have a TCR which is composed of one alpha (α) and one beta (β) glycoprotein chain. The TCR of the γδ T cells is characterized by the expression of one gamma (γ) and one delta (δ) molecule chain (Thome et al. 1994; Gerner et al. 2009). For antigen recognition the two chains typically form a heterodimer (Figure 2).

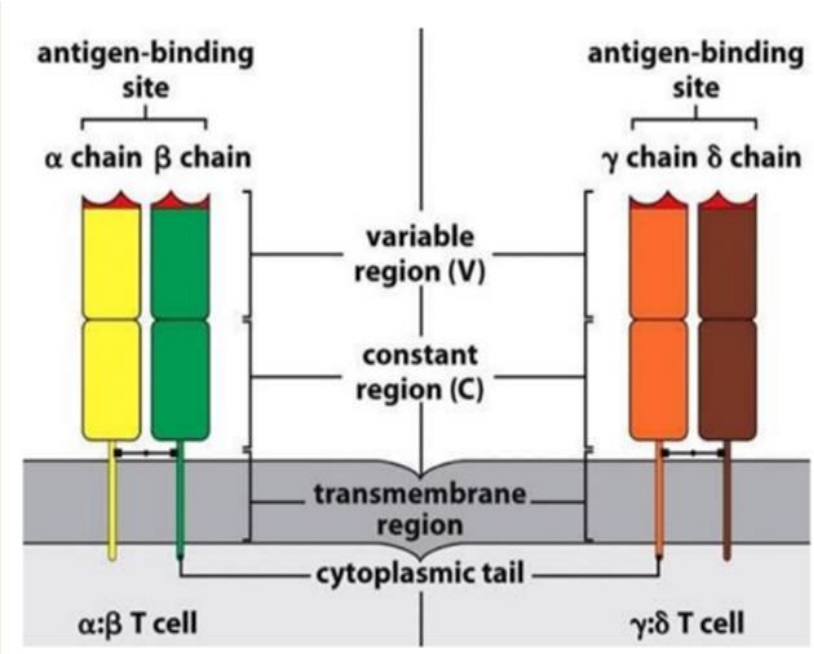

Figure 2: The two classes of TCR
The figure shows the two different classes of the T-cell receptor. The TCR of αβ T cells has an α and a β chain. The TCR of γδ T cells is composed of a γ and a δ peptide chain.
From: The Immune system, 3rd edition (Garland science 2009)

The αβ T cells can be further phenotypically divided into $CD4^+CD8^-$, $CD4^+CD8^{lo}$, $CD4^-CD8^{lo}$ and $CD4^-CD8^{hi}$ T cells. Especially here, the existence of extrathymic cells expressing both CD4 and CD8 is a peculiarity of swine (Saalmüller et al. 1987). The γδ T cells are categorized in $CD2^+CD4^-CD8^-$, $CD2^+CD4^-CD8^{lo}$ and $CD2^-CD4^-CD8^-$ cell subsets (Charerntantanakul and Roth 2006) (Figure 3). One of the most significant differences between αβ T cells and γδ T cells in terms of their function, is their antigen recognition. While αβ T cells need a presentation of the antigens via the MHC, the γδ T cells can recognize antigens in an MHC non-restricted fashion (Charerntantanakul and Roth 2006; Takamatsu et al. 2006). $CD4^+$ αβ T cells detect antigens presented in MHC-class-II molecules and $CD4^-CD8^+$ αβ T cells can only identify antigens presented in MHC-class-I molecules (Saalmüller et al. 1999; Charerntantanakul and Roth 2006; Gerner et al. 2009).

T cell subpopulation	MHC restriction	Response to antigens
αβ T cells		
$CD4^+CD8^-$	MHC class II	Cell proliferation Up-regulation of CD8 Up-regulation of MHC class II
$CD4^+CD8^{lo}$	MHC class II	Up-regulation of CD25 Cell proliferation Cytokine secretion Stimulation of B cells
$CD4^-CD8^{lo}$	MHC class I	Unknown
$CD4^-CD8^{hi}$	MHC class I	Up-regulation of CD25 Cell proliferation Cytokine secretion Cell cytotoxicity
γδ T cells		
$CD2^+CD4^-CD8^-$	No	Cell proliferation Cytokine secretion
$CD2^+CD4^-CD8^{lo}$	No	Cell proliferation Cytokine secretion Cell cytotoxicity
$CD2^-CD4^-CD8^-$	No	Unknown

Figure 3: Summary of characteristics of porcine T cell subpopulations
The figure shows the division into porcine T cell subpopulations, their MHC restriction, and the corresponding cellular processes after antigen stimulation.
From: Charerntantanakul and Roth 2006, p. 83

1.4.3 Porcine αβ T cells

1.4.3.1 $CD4^+$ T helper cells

Porcine $CD4^+CD8^-$ αβ T cells are referred to as naïve T helper (Th) cells since they have not yet had contact with foreign antigens. After antigen contact, they begin to proliferate and upregulate expression of MHC-class-II and CD8 molecules. Therefore, CD8 expression on $CD4^+$ T cells marks antigen-experienced cells (Saalmüller et al. 2002). Importantly, here CD8 is expressed in the αα homodimer form (Yang and Parkhouse 1997; Gerner et al. 2009). Furthermore, CD8α together with CD27 can be used to distinguish central and effector memory cells (Reutner et al. 2012; 2013). The main functions of the $CD4^+CD8^+$ memory Th cells is the recognition of recall antigens and the subsequent production of specific cytokines (e.g. Interferon (IFN) α, IL-2 or IFN-γ) (Reutner et al. 2013; Talker et al. 2015). The presence of the CD8α molecule is a suitable tool to differentiate $CD4^+CD8^+$ memory Th cells from $CD4^+CD8^-$ naïve Th cells (Saalmüller et al.2002).

1.4.3.2 Cytolytic T cells

The $CD4^-CD8^+$ T cells are also referred to as cytolytic T cells (CTL). They represent a very important type of immune cell and are characterized by the recognition of foreign antigens in an MHC-class-I restricted manner (Yang and Parkhouse 1997). Subsequently, they can kill target cells with perforins and granzymes or secrete cytokines such as IFN-γ or TNF-α to initiate immune response (Charerntantanakul and Roth 2006; Denyer et al. 2006). Porcine cytolytic T cells are characterized by expression of CD8 as αβ heterodimer (Gerner et al. 2009). It was shown that they play an important role in viral infections like influenza A (Talker et al. 2015) or African Swine Fever (Martins et al. 1993). Very recently transcriptome analysis revealed in-depth details on porcine naïve and memory CTL subsets (Lagumdzic et al. 2022).

1.4.4 Porcine γδ T cells

The γδ T cells are one of the major T-cell subpopulation in the peripheral blood lymphocytes (PBL) of pigs (Yang and Parkhouse 1996; Talker et al. 2013). The phenotypic classification is based on the division into $CD2^+$ and $CD2^-$ γδ T cells. Due to CD8 expression, the $CD2^+$ γδ T cells represent two additional subgroups ($CD2^+CD8^-$ and $CD2^+CD8^+$ γδ T cells) with different functional properties like production of different cytokines (Sedlak et al. 2014). One of the most important features of these two subpopulations, is the recognition of antigens in a non MHC

restricted manner. The antigen stimulation is followed by cell proliferation and an expression of cytokines (Takamatsu et al. 2006). Like NK cells, they also express the CD8 receptor in the form of an αα homodimer (Yang and Parkhouse 1997; Gerner et al. 2009).

1.5 Natural killer (NK) cells

NK cells are a subpopulation of lymphocytes, that play an important role in the early immune response. Their functions include the killing of virus-infected cells and tumours, as well as the production of immune-regulatory cytokines (e.g., IFN-γ and TNF-α) (Moretta et al. 2008). NK cells develop from lymphoid stem cells in the bone marrow and are then released into the bloodstream. They do not have antigen-specific receptors on their cell surface like T and B cells, but instead express germ-line encoded receptors (Moretta et al. 2008). The activity of NK cells is stimulated by interferons or cytokines, which are secreted by macrophages. The cytoplasm of NK cells contains numerous small granules consisting of proteins, such as perforins or proteases (e.g. granzymes). They are released in the vicinity of target cells, where they lead to perforation of the cell membrane and induction of apoptosis. Activation of NK cells is regulated by two forms of surface receptors - activating and inhibitory receptors. These receptors interact with molecules of the MHC-class-I molecule on the surface of the target cells (inhibitory signal) but also stress-induced ligands (activating signal) (Moretta et al. 2008).

Phenotyping of porcine NK cells can only be made possible by specific marker combinations (e.g., CD8α vs. CD16 and CD8α vs CD3), since individual selective markers are still missing (Mair et al. 2014). Initially porcine NK cells were defined by specific marker combinations and were described by a perforin$^+$ CD2$^+$ CD3$^-$ CD4$^-$ CD5$^-$ CD6$^-$ CD8α$^+$CD8β$^-$CD16$^+$ phenotype (Denyer et al. 2006). Phenotyping furthermore confirms that porcine NK cells only express the CD8 receptor molecule in the form of CD8α homodimer chains (Gerner et al. 2009). More recently, it was described that porcine NK cells can be divided into distinct functional subsets based on different expression levels of the activating receptor NKp46 and CD8α (Mair et al. 2012; 2013).

1.6 Antibody structure and monoclonal antibodies (mAbs)

Monoclonal antibodies are immunologically active proteins produced by B cells or B-cell lines. They are generated by cloning a unique precursor B lymphocyte. In comparison to the typical polyclonal antibodies, a mAb is directed only against one specific epitope of an antigen. In diagnostics and research, mAbs have become a very important tool to detect many molecules with a high specificity in techniques like immunohistochemistry and flow cytometry. The general production of mAbs is based on the fusion of antibody-producing B-cells with cells of a myeloma cell line, resulting in hybrid cells, that produce indefinitely antibodies of one specificity (Köhler and Milstein 1975). For the final extraction of the mAbs, the hybridoma cell line, that best produces antibodies that bind to the desired epitope of a specific antigen is selected (Posner et al. 2019; Nelson et al. 2000).

The molecular structure of antibodies depends on their class. In most mammals, there are five different classes (isotypes) of immunoglobulins (IgA, IgG, IgD, IgE, IgM), which are classified based on their different gene segments for the constant parts of the heavy chains. The general antibody structure is composed of two identical heavy chains and two identical light chains. The polypeptide chains are connected to each other by covalent disulfide bonds and arranged in the form of a "Y". Each chain is comprised of constant (C_L, C_H1, C_H2, C_H3) and variable domains (V_L, V_H). In contrast to light chains, heavy chains have three different constant regions (C_H1, C_H2, C_H3). The variable domains of one light chain and one heavy chain together form the antigen binding site (F_v) (Posner et al. 2019; Ma and O'Kennedy 2015). The exceptional variability of antigen binding sites (Complementarity Determining Region (CDR)) is achieved by the organism through V(D)J recombination. This is an intentional genetic DNA rearrangement process, in which the gene segments V, D and J are recombined to produce a variety of new antibodies and receptors with unique antigen specificity (Chi, Li, and Qiu 2020). Together with the constant regions of the light chains and the first constant regions (C_H1) of the heavy chains, this forms the so-called Fab (antigen-binding fragment). The Fab is also called the V part of the Y-shaped antibody. The lower part, consisting only of residual constant domains of heavy chains, is generally described as the Fc (constant fragment) fragment. This part can interact with components of the complement system or bind to the Fcγ receptors on the

effector cells of the innate immune system (Posner et al. 2019; Ma and O'Kennedy 2015). Figure 4 gives an overview of the general antibody structure.

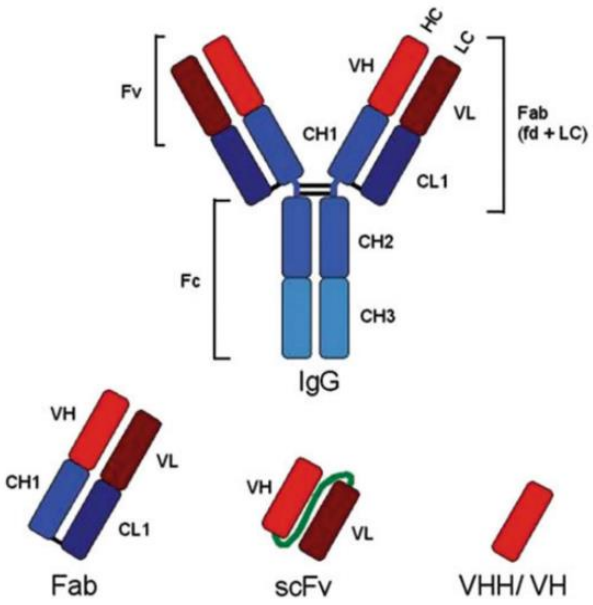

Figure 4: Illustration of an IgG and the structural units of IgGs
The figure shows the typical components of an immunoglobulin class G (IgG). The upper part is commonly known as the antigen-binding fragment (Fab), consisting of variable and constant regions of the light and the heavy chains. The lower part consists exclusively of constant regions of the heavy chains and is therefore referred to as constant fragment (Fc). From: Posner et al. 2019, p.7

1.7 Aim of the study

Preliminary results indicate that distinct combinations of mAb clones for porcine CD8α and CD8β chains can cause troubles in multi-color staining panels. It is assumed that the binding of the anti-CD8α 11/295/33 mAb clone to the CD8α chain complicates the binding of the anti CD8β PPT23 and PG164A mAb clone to the CD8β chain by a form of steric hindrance. This can lead to suboptimal detection of $CD8\beta^{+}$ cells. Therefore, the aim of the study was to search for an mAb composition that is suitable for the simultaneous detection of CTLs (defined by the CD8β phenotype) in combination with lymphocyte subsets expressing the CD8αα homodimers (such as NK cells, γδ T cells, or CD4+ antigen-experienced T cells). The obtained data will help in future panel designs for multi-colour flow cytometry in the pig and therefore improving studies of porcine immune cells.

2 Material and Methods

2.1 Material

2.1.1 Reagents and solutions

Table 1: Reagents and solutions used during the work

Reagent/Solution	**Manufacturer/Company**
PBS (without Ca^{2+}, Mg^{2+})	PAN-Biotech (Aidenbach, Germany)
Lymphocyte separation medium (Pancoll human, density 1.077 g/ml)	PAN-Biotech
Washing Medium: RPMI 1640 with stable glutamine 5 % (v/v) FCS 100 IU/ml penicillin 0.1 mg/ml streptomycin	 PAN-Biotech Sigma-Aldrich (Missouri, USA) PAN-Biotech PAN-Biotech
Tissue Culture Medium: RPMI 1640 with stable glutamine 10 % (v/v) FCS 100 IU/ml penicillin 0.1 mg/ml streptomycin	 PAN-Biotech Sigma-Aldrich PAN-Biotech PAN-Biotech
Freezing Medium: RPMI 1640 with stable glutamine 100 IU/ml penicillin 0.1 mg/ml streptomycin 40 % (v/v) FCS 10 % (v/v) DMSO	 PAN-Biotech PAN-Biotech PAN-Biotech Sigma-Aldrich Sigma-Aldrich
FCM buffer: PBS (without Ca^{2+}, Mg^{2+}) 10 % (v/v) heat inactivated porcine plasma	 PAN-Biotech Obtained in-house

2.1.2 Antibodies

The following antibodies were used for the experiments performed in the thesis.

Table 2: Primary antibodies for cell surface antigens

Antigen	Fluorochrome	Clone	Isotype	Conjugated	Source
CD3		BB23-8E6	Mouse IgG2b	Indirect*	Southern Biotech (Birmingham, USA)
CD8α		76-2-11	Mouse IgG2a	Indirect*	In-house conjugated
CD8α	PE	76-2-11	Mouse IgG2a	Direct	BD Bioscience (New Jersey, USA)
CD8α		11/295/33	Mouse IgG2a	Indirect*	
CD8α	Alexa Fluor 647	11/295/33	Mouse IgG2a	Direct	In-house conjugated
CD8α	Alexa Fluor 488	11/295/33	Mouse IgG1	Direct	
CD8α	PE	295/33/25	Mouse IgG2a	Direct	BD Bioscience
CD8β		PPT23	Mouse IgG1	Indirect*	
CD8β	Alexa Fluor 488	PPT23	Mouse IgG1	Direct	In-house conjugated
CD8β		PG164A	Mouse IgG2a	Indirect*	Kingfisher Biotech (Minnesota, USA)
CD8β	Alexa Fluor 647	PG164A	Mouse IgG2a	Direct	Kingfisher Biotech, in-house conjugation

*The corresponding secondary antibodies are listed in Table 3

Table 3: Secondary antibodies

Target Species	Isotype specificity	Fluorochrome	Antibody host species	Producer
Rat-anti mouse	IgG1	Brilliant Violet 421	Rat IgG monoclonal Clone RMG1-1	BioLegend (San Diego, USA)
Goat-anti mouse	IgG1	Alexa Fluor 488	Polyclonal goat	Thermo Fisher Scientific (Waltham, USA)
Goat-anti mouse	IgG2a	Alexa Fluor 647	Polyclonal goat	Jackson Immuno Research (Pennsylvania, USA)
Goat-anti mouse	IgG2a	PE-Cy7	Polyclonal goat	Southern Biotech
Goat-anti mouse	IgG2b	Alexa Fluor 488	Polyclonal goat	Jackson Immuno Research
Goat-anti mouse	IgG2b	Brilliant Violet 421	Polyclonal goat	Jackson Immuno Research

The following dye was used to label the dead cells.

Table 4: Live/dead stain

Live/dead stain	Producer
Fixable Viability Dye eFluor780	Thermo Fisher Scientific

2.1.3 Devices and instruments

Table 5: Devices, instruments and softwares used during the work

Product name	Company	Company headquarter
Heraeus megafuge 40R universal centrifuge	Thermo Fisher Scientific	Waltham, USA
Sysmex XP-300 cell counter machine	Sysmex	Kobe, Japan
CytoFLEX LX Flow Cytometer	Beckman Coulter Life Sciences	Brea, USA
FlowJo Software version10.8.1	BD Biosciences	New Jersey, USA
GraphPad PRISM Software version9.5.1	Dotmatics	Boston, USA

2.1.4 Animals and cellular material

The samples of porcine blood for the isolation of lymphocytes needed for the experiments, were obtained from six-to-seven-month-old healthy pigs from a slaughterhouse in Lower Austria. Animals underwent electric high-voltage anaesthesia and subsequent exsanguination in accordance with the Austrian Animal Welfare Slaughter Regulation. Whole blood was collected in beakers with heparin solution to prevent clotting of blood.

2.2 Methods

2.2.1 Isolation of porcine Peripheral Blood Mononuclear Cells

The isolation of porcine peripheral blood mononuclear cells (PBMCs) was performed as followed:

In the first step, the heparinized blood was diluted with phosphate buffered saline (PBS) in a ratio of 1:1. Subsequently, 35 ml of the blood dilution was overlayed on 15 ml of lymphocyte separation medium (LSM) in sterile 50 ml conical tubes. Centrifugation was performed at room temperature (RT) for 30 minutes at 920 × g. This led to a typical separation consisting of a plasma phase at the top, the required peripheral blood mononuclear cells (lymphocytes and monocytes) in the middle, followed by the LSM (frequently referred to as Ficoll gradient) and the erythrocytes (red blood cells) at the bottom (Figure 5).

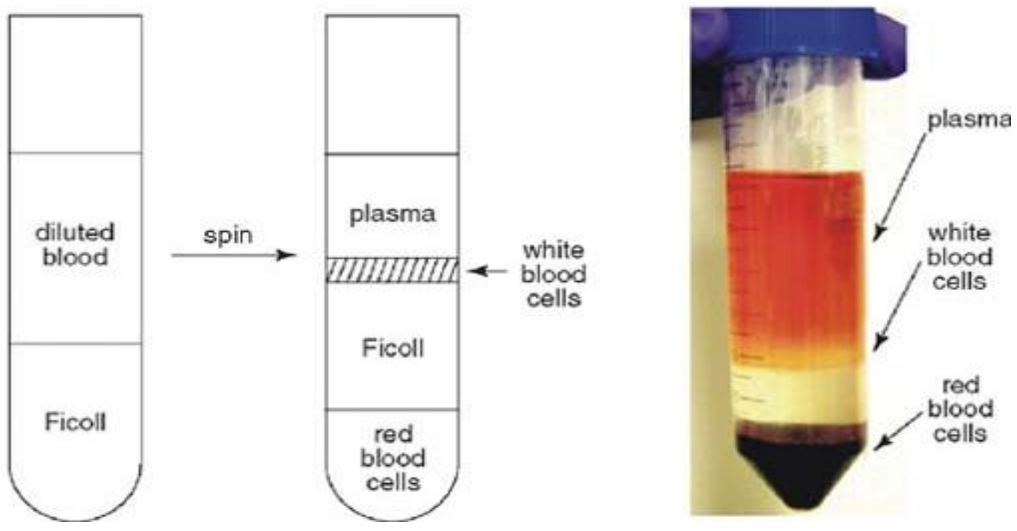

Figure 5: Isolation of PBMCs using density gradient centrifugation.
The figure shows the separation of blood after density gradient centrifugation into a plasma phase, a leukocyte phase, the Ficoll gradient and a settled erythrocyte phase at the bottom.
From: mca04c-fig-0002-1-full.jpg (535×315) (wiley.com)

The desired PBMCs could then be aspirated by using a 5 ml pipette and were transferred into prepared tubes with ice-cooled PBS. The tubes were filled with cold PBS and centrifugated at 4 °C for 10 minutes at 470 × g. After removing the supernatant and resuspending the cells with residual PBS, cells of the same animal were pooled into one tube. The tube was filled up with PBS and centrifuged as described before. The supernatant was removed and after resuspending the cells with residual PBS, the centrifugation step was repeated one more time with cold wash medium. After this last step, cells were resuspended in cold culture medium and were ready for cell count. Cell counting was performed by using a cell counter machine (Sysmex XP 300 Sysmex, Japan).

2.2.2 Cryo-preservation of porcine PBMCs

Cells were cryo-preserved in order to store them for later use. In a first step, the number of required cryo-vials from total cell number had to be calculated. A single cryo-vial included cells in a range from 3×10^7 up to 6×10^7 PBMCs. After centrifugation (8 minutes at 470 × g and 4 °C), the supernatant was discarded, and the cells were resuspended in ice-cold freezing medium. The cell suspension was then distributed in 1 ml aliquots into pre-cooled cryo-vials. Subsequently, they were stored in a -80 °C freezer for short term storage. After 24-48 hours cells were moved to a -150 °C freezer for long term storage.

2.2.3 Defrosting of porcine PBMCs

To thaw the required cells, they were taken out the freezer and directly placed in a water bath heated up to 37 °C. After the cell suspension was melted, 1 ml of FCM buffer was added and the whole suspension was transferred to a 15 ml conical centrifuge tube, containing approximately 10 ml of pre-warmed FCM buffer. After centrifugation (8 minutes at 470 × g and RT), the supernatant was discarded, and the cells were resuspended in 2 ml FCM buffer. For the following cell counting, 100 µl of the cell suspension were removed and measured with the Sysmex XP-300 cell counter machine as described above.

2.2.4 Flow cytometry

Flow cytometry (FCM) is an established method in the field of laboratory medicine. It is mainly used to characterize cells according to their phenotypic properties. A cell suspension flows through a thin measuring chamber and is irradiated with laser light**.** This creates so-called

scattered light signals, which are measured together with the autofluorescence of the cells by specific detectors (Figure 6). A computer converts the light signals into electrical signals and displays them graphically. Subsequently, a statement can be made about the distribution and the number of the different cell populations in the sample. Fluorescent reagents used in FCM include fluorescent conjugated antibodies, DNA binding dyes, viability dyes or fluorescent expression proteins. Fluorochrome-labeled antibodies that specifically bind to antigens of interest can be used to detect surface or intracellular molecules. Each cell is examined for visible light scattering and one or more fluorescence parameters. The scatter of visible light is measured in two different directions. The forward direction (Forward scatter or FSC) provides an indication of the relative size of the cell. The sideward direction (Sideward scatter or SSC) indicates the internal complexity or granularity of the cell (Adan et al. 2017; McKinnon 2018).

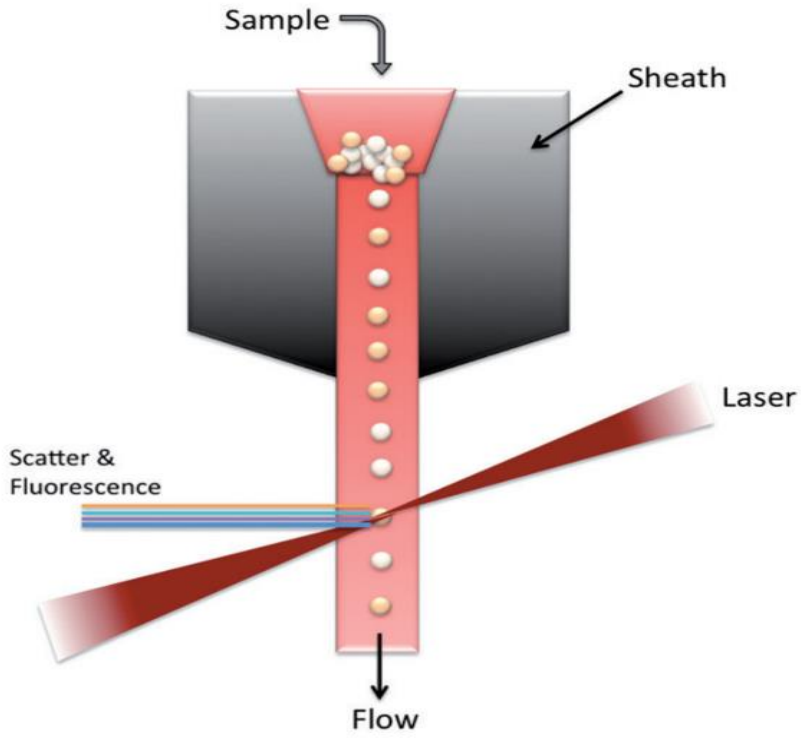

Figure 6: The underlying working principle of a flow cytometer
The figure shows the typical elements of flow cytometric measurements. The cells move through the flow cytometer in a buffered salt-based solution and are successively irradiated with lasers. The emitted cell specific light signals are perceived by the responsible detectors.
From: Adan et al. 2017, p. 164

2.2.4.1 FCM staining in microtiter-plates

Thawed PBMCs were resuspended in FCM buffer and prepared for the staining of the flow cytometric analyses. The required cell count was between 1×10^6 and 2×10^6 cells per sample. Depending on the concentration of the cell suspension, a calculated volume was added to 96 well round-bottom microtiter plates (one well per sample). After centrifugation (4 minutes at 470 × g and 4 °C), the supernatant was discarded. Then the primary antibodies were added and after mixing, it was incubated in the fridge for 20 minutes. After this time, cells were washed with 200 µl of FCM buffer to remove residual antibodies. The buffer was added, and the plate was centrifugated with the same settings as before. Then the supernatant was removed, and the cell pellet was resuspended. The washing step was always repeated two times after every incubation. Subsequently, the secondary antibodies could be added. The incubation and washing process was performed as described above. Before measuring the samples on the flow cytometer, cells were resuspended with 250 µl of FCM buffer. The measurement was then carried out in the microtiter plate itself or the cell solution was filled into FCM tubes. The evaluation of the data was performed on the flow cytometer CytoFLEX LX (Beckman Coulter USA) and the final analysis, as well as the graphical display, was accomplished with the help of the software FlowJo (Becton Dickinson Biosciences, USA). At least 1×10^5 cells were recorded per sample. The graphs for the presentation of the results were additionally created with a statistic tool (GraphPad PRISM, Dotmatics, USA).

Due to high heterogeneity in data of individual animals no further statistics were performed. This will be done after analysing more animals in follow-up experiments.

3 Results

After flow cytometric measurements, the samples had to be processed using FlowJo Software. In the first step, lymphocytes were selected according to the sidewards and the forwards scatter area (SSC-A and FSC-A). Subsequently, cells that stuck together, so-called cell doublets, were excluded to avoid false results. In this case, the forward scatter height (FSC-H) was juxtaposed to the FSC-A. Lastly, the dead lymphocytes were excluded from the living ones by gating on viability dye negative cells. This gating procedure was used in all experiments (Figure 7).

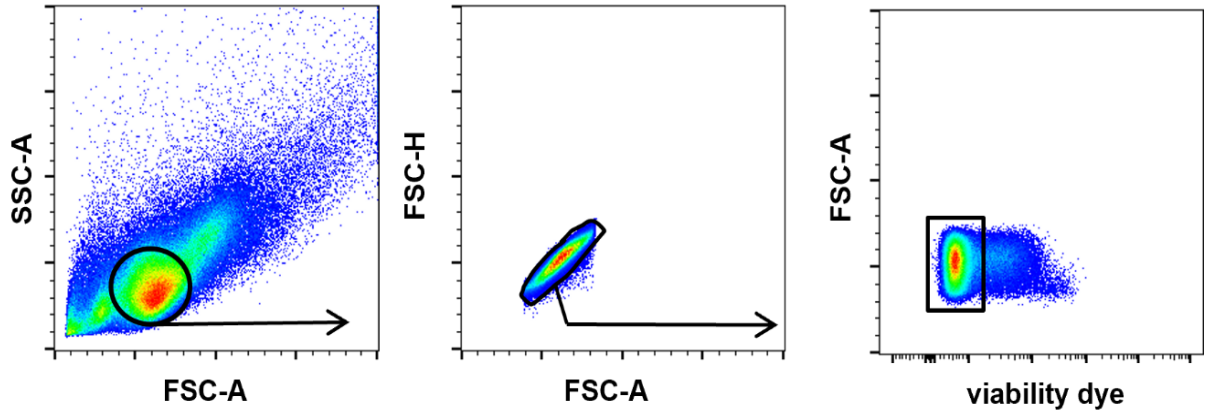

Figure 7: Gating strategy
The lymphocyte population was selected for experimental evaluation. Within the lymphocytes (FSC-A/SSC-A), cell duplicates were sorted out (FSC-A/FSC-H). From the single lymphocytes, the dead cells were excluded (viability dye negative).

3.1 CD8α and CD8β co-staining experiments

As part of the thesis, several experiments were performed to investigate the interactions between different CD8α and CD8β binding mAb clones. The experiments were performed with samples of at least four different animals. The following Figures (8-12) show how the resulting CD8β-associated FCM signal changes depending on the time of addition of the respective CD8α binding mAb clones.

First, the effects of a co-staining with the anti-CD8α 11/295/33 mAb clone on the anti-CD8β PPT23 mAb clone were evaluated (Figure 8). The aim was to examine the binding of the PPT23 clone by adding the 11/295/33 clone at different timepoints in the staining (colour-coded groups in Figure) and to evaluate the resulting population size and signal strength caused by the CD8β binding PPT23 mAb clone. As co-staining, the pan T-cell marker CD3 was selected using the anti-CD3 BB23-8E6 mAb clone and the secondary antibody anti-IgG2b-Alexa488. The first

group analysed was the control group (w/o, red boxplots) and showed a staining with the PPT23 clone only, without CD8α. In the next group the 11/295/33 clone was simultaneously added with the PPT23 clone (simultaneous, orange boxplots). The third group included the addition of the 11/295/33 clone approximately 20 minutes before the addition of the PPT23 clone (alpha before, green boxplots). This process was also measured the other way round, where the PPT23 clone was added at least 20 minutes before the 11/295/33 clone (alpha after, light blue boxplots). In the last group, the 11/295/33 clone was added to the PPT23 clone with a delay of about only five minutes (alpha delayed, dark blue boxplots). This system was also used in the following experiments only with other mAb clones for the CD8α and the CD8β chain. Binding of the PPT23 clone was measured using the secondary antibody anti-IgG1-Brilliant Violet 421. The pseudo-colour plots in Figure 8A represent the lymphocytes of a single representative animal and display CD8β on the x-axis and CD3 on the y-axis. The $CD3^+CD8\beta^+$ cell populations are outlined by a rectangle gate. The boxplots show the frequencies of $CD8\beta^+$ lymphocytes (Figure 8B) and the median fluorescence intensity (MFI) of $CD8\beta^+$ cells (Figure 8C) of all animals analysed. In addition, the samples of individual animals used in every experiment are represented by different symbols (circle, square, triangle, diamond, asterisk). This form of data presentation was also used in following experiments (Figures 9-12).

The median of the tested animals for the frequencies and MFI of CD8ß within the different groups is given as a comparative value. In contrast to the sample without the anti-CD8α mAb (w/o, %: 15.3 / MFI: 50265), addition of the 11/295/33 clone caused a significant decrease in the resulting PPT23 CD8β signal as the frequencies of $CD8\beta^+$ lymphocytes generally decreased with simultaneous (%: 10.70 / MFI: 13978) and prior (%: 5.61 / MFI: 2531) addition of the 11/295/33 clone. The addition of the 11/295/33 clone to the PPT23 clone after 20 minutes (%:14.10 / MFI: 28420) and the delayed addition after five minutes (%: 14 / MFI: 30607) both resulted in similar percentages of $CD8\beta^+$ lymphocytes in comparison to the control group in every animal tested. Regarding the MFI of CD8β the overall same phenomena could be observed, although the MFI could not be completely restored in the “alpha after” and “alpha delayed” group.

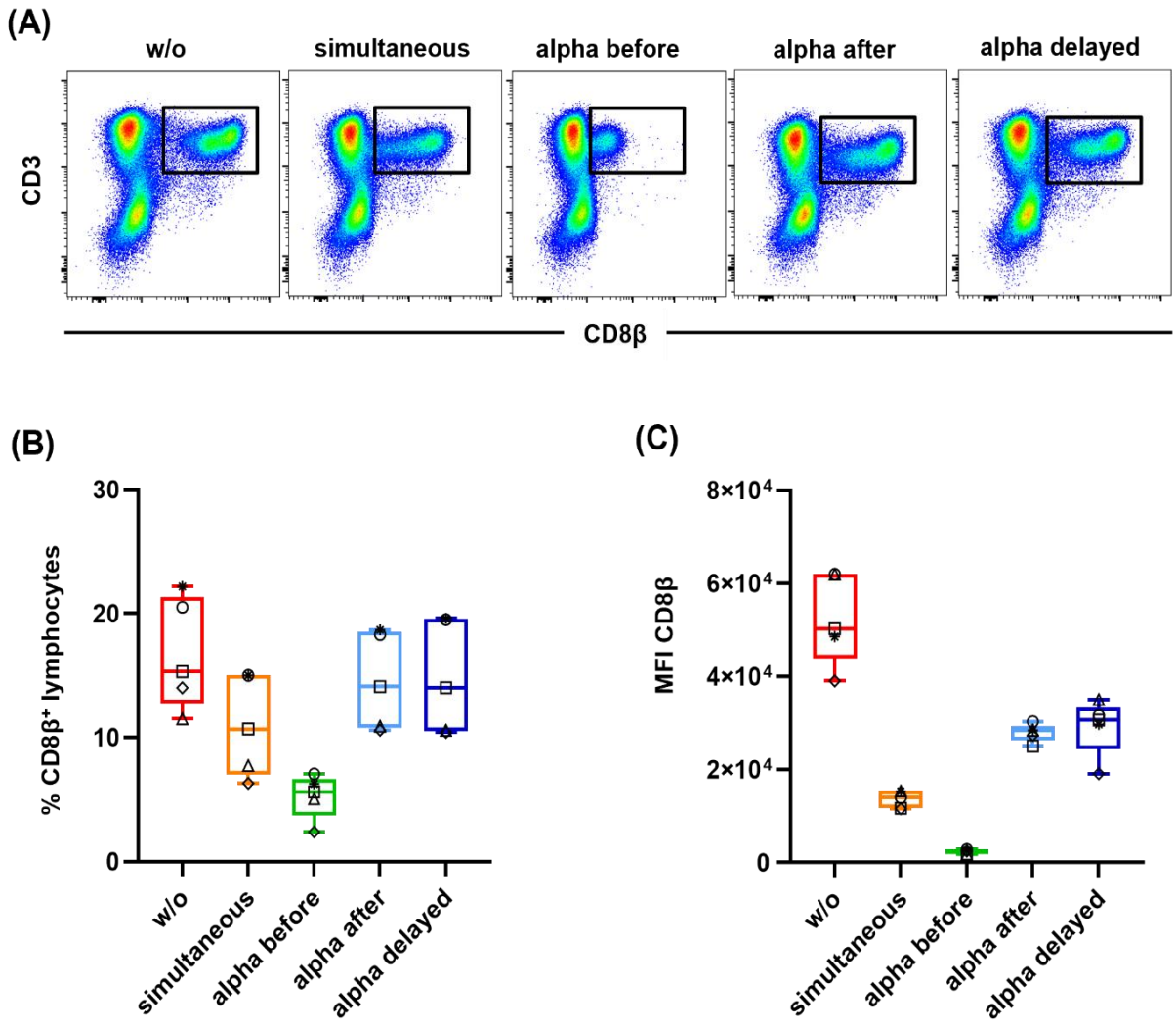

Figure 8: The effects of the 11/295/33 clone on the PPT23 clone
The figure shows the effects of adding the anti-CD8α 11/295/33 mAb clone to the anti-CD8β PPT23 mAb clone at different timepoints (colour-coded groups) in terms of the resulting CD8β signal strength. The pseudo-colour plots represent the lymphocytes of a single representative animal (A). The experiment was performed with samples from five different animals. In the boxplots the frequencies of $CD8\beta^+$ lymphocytes (B) and the MFI of CD8β (C) are shown. Individual tested animals are represented by different symbols (circle, square, triangle, diamond, asterisk). The middle line of each boxplot indicates the median of the tested animals for every group.

In the second experiment, the influence of the anti-CD8α 76-2-11 mAb clone on the anti-CD8β PPT23 mAb clone was investigated. The procedure was analogous to the first experiment and the results were presented in the same way as described above. To detect CD8β chain binding, the secondary antibody anti-IgG1, labelled with the fluorochrome Brilliant Violet 421 was used. From the pseudo-colour plots we concluded that the CD8β signal did not visibly change by the addition of the 76-2-11 mAb clone (Figure 9A). The frequencies of $CD8\beta^+$ lymphocytes were

highest in the control group in every animal tested (w/o, %: 20.8 / MFI: 40410) but did not obviously decrease by the different treatments with the 76-2-11 clone in all animals investigated (%: 18.2-20.8) (Figure 9B). The same could be observed for the MFI signal of CD8β (MFI: 27204-40410) (Figure 9C). In this experiment, it seemed that it had no significant influence at which time-point the 76-2-11 clone was added to the PPT23 clone.

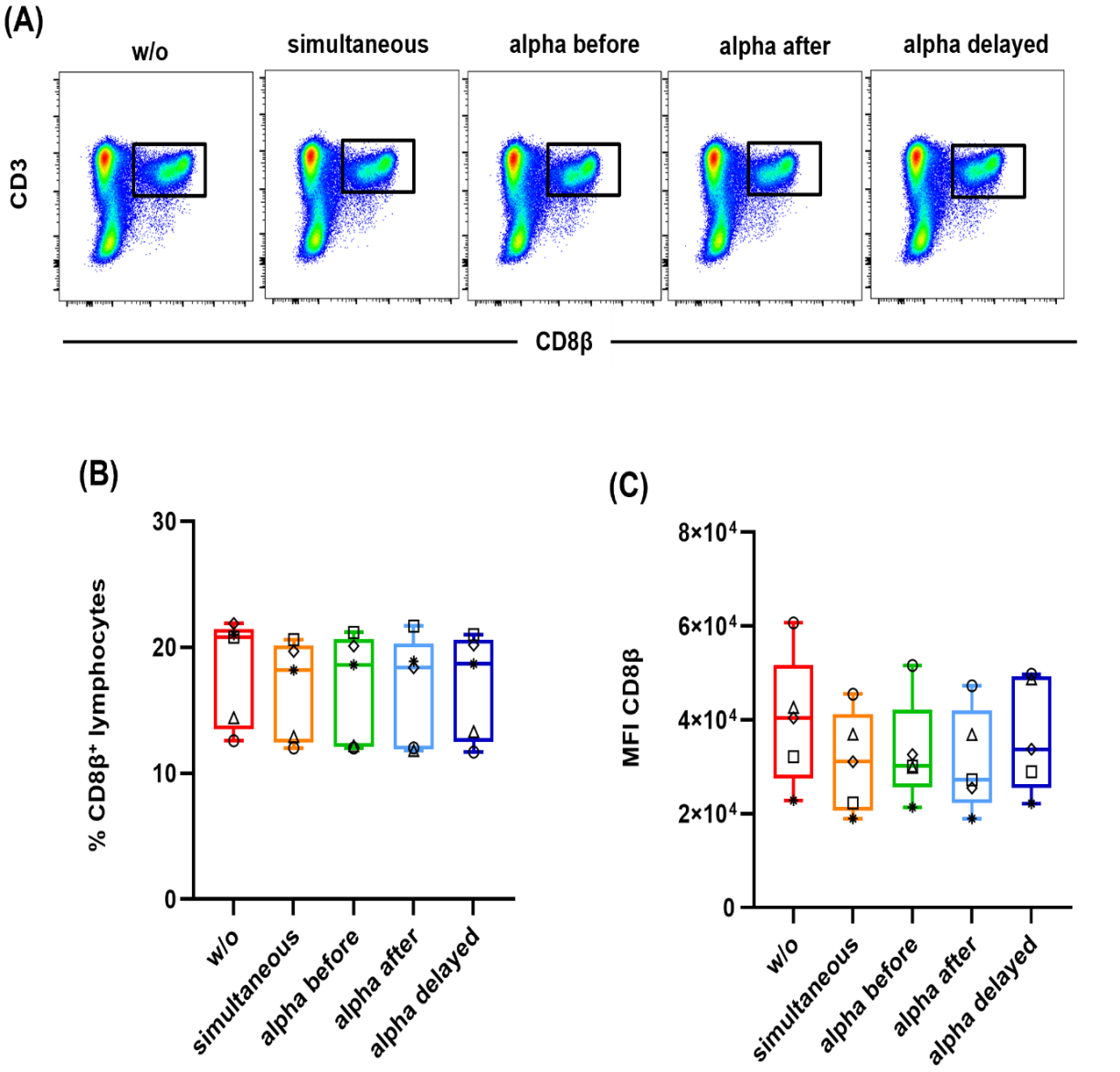

Figure 9: The effects of the 76-2-11 clone on the PPT23 clone
The figure shows the effects of adding the anti-CD8α 76-2-11 mAb clone to the anti-CD8β PPT23 mAb clone at different timepoints (colour-coded groups) in terms of the resulting CD8β signal strength. The pseudo-colour plots represent the lymphocytes of a single representative animal (A). The experiment was performed with samples from five different animals. In the boxplots the frequencies of $CD8\beta^+$ lymphocytes (B) and the MFI of CD8β (C) are shown. Individual tested animals are represented by different symbols (circle, square, triangle, diamond, asterisk). The middle line of each boxplot indicates the median of the tested animals for every group.

The third experiment involved the study of the interactions between the anti-CD8α 11/295/33 mAb clone, directly labelled with the fluorochrome Alexa-647 and the anti-CD8β PPT23 mAb clone, directly labelled with the fluorochrome Alexa-488. This experiment was performed with directly labelled mAbs to exclude possible influences of an indirect staining thus involving secondary antibodies in binding capacities of the primary mAb clones. Like in the first experiment (Figure 8), the pseudo-colour plots indicated a strong decrease of the CD8β signal when adding the 11/295/33 clone simultaneous and 20 minutes before the PPT23 clone in comparison to the control group. The box plots considering the frequencies of $CD8\beta^+$ lymphocytes and the MFI of CD8β confirmed these phenomena and showed similar behaviour.

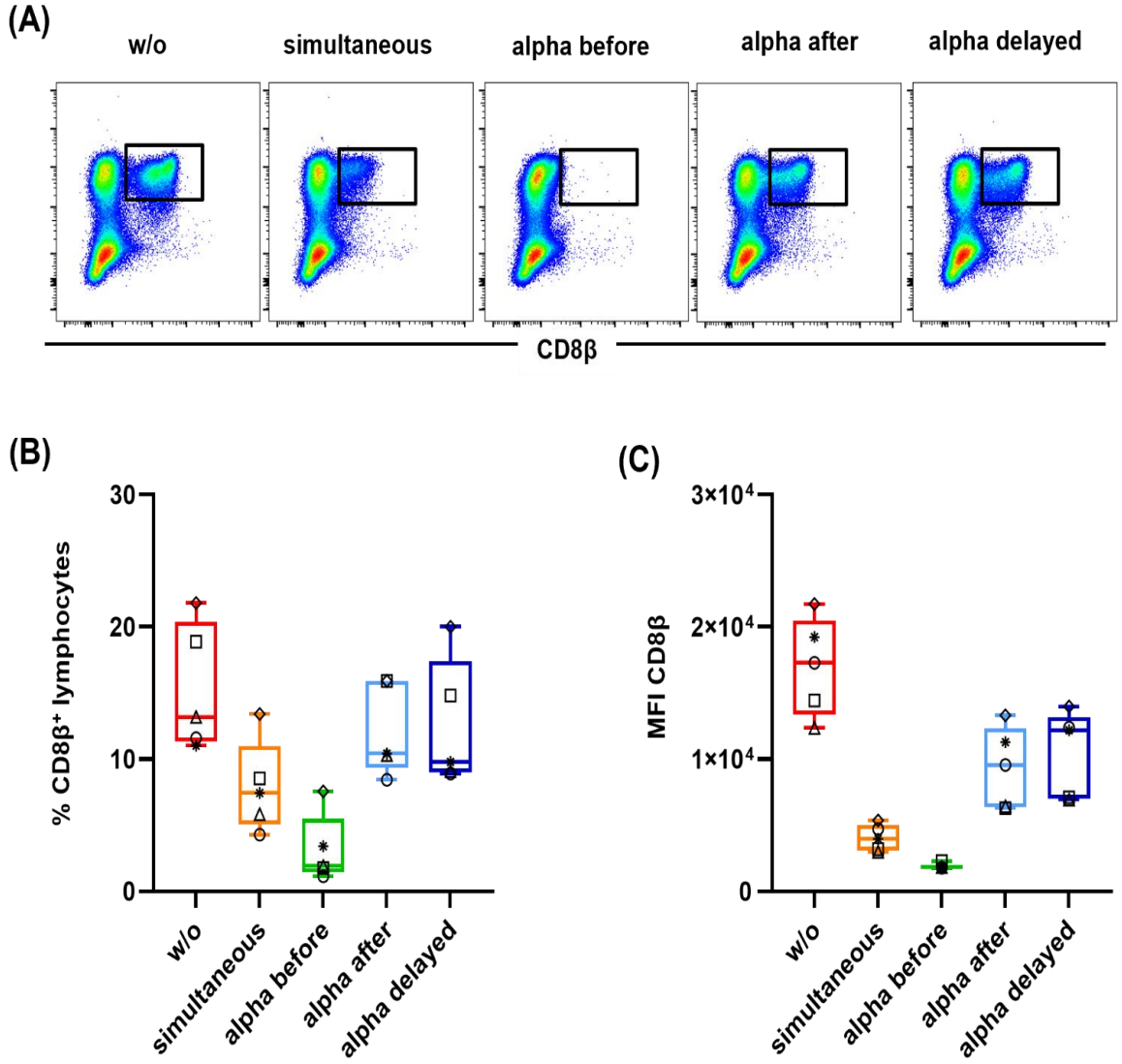

Figure 10: The effects of the 11/295/33 clone on the PPT23 clone (directly labelled)
The figure shows the effects of adding the directly labelled anti-CD8α 11/295/33 mAb clone to the directly labelled anti-CD8β PPT23 mAb clone at different timepoints (colour-coded groups) in terms of the resulting CD8β signal strength. The pseudo-colour plots represent the lymphocytes of a single representative animal (A). The experiment was performed with samples from five different animals. In the boxplots the frequencies of $CD8\beta^+$ lymphocytes (B) and the MFI of CD8β (C) are shown. Individual tested animals are represented by different symbols (circle, square, triangle, diamond, asterisk). The middle line of each boxplot indicates the median of the tested animals for every group.

The control group had the highest average values in every animal tested (w/o, %: 13.2 / MFI: 17295) and the previous addition of the 11/295/33 clone led to the smallest values (%: 1.91 / MFI: 1823).Simultaneous addition of the 11/295/33 and the PPT23 clone resulted in the second smallest values (%: 7.43 / MFI: 3954) considering the frequencies of $CD8\beta^+$ lymphocytes and the MFI of CD8β. Although addition of the 11/295/33 clone after the PPT23 clone led to a better CD8β signal, it was reduced compared to the staining without the anti-CD8α mAb. However, whether the 11/295/33 clone was added 20 (%: 10.4 / MFI: 9564) or only five minutes (%: 9.78 MFI: 12198) after the PPT23 clone, did not make an appreciable difference (Figure 10A-C).

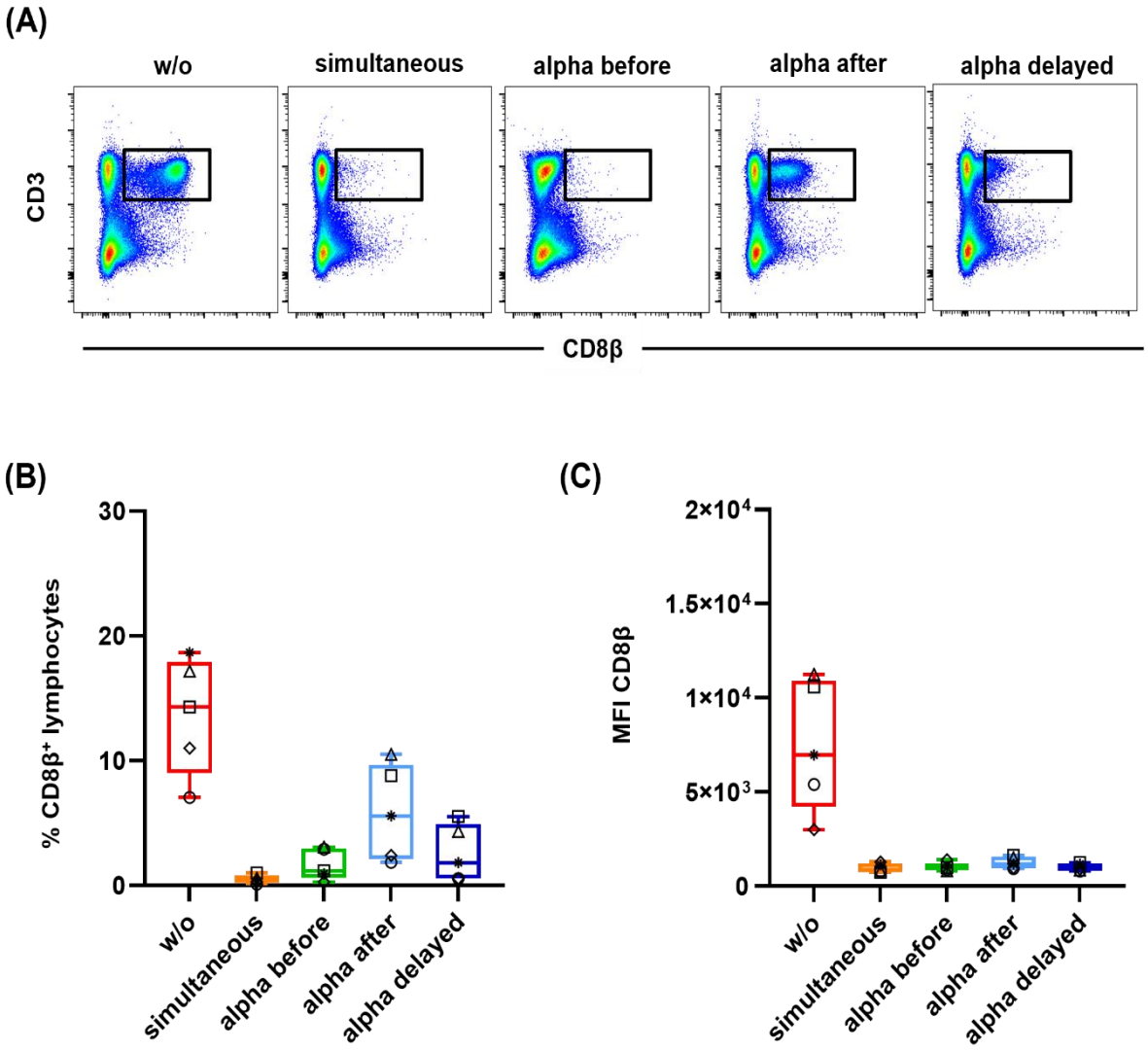

Figure 11: The effects of the 11/295/33 clone on the PG164A clone
The figure shows the effects of adding the anti-CD8α 11/295/33 mAb clone to the anti-CD8β PG164A mAb clone at different timepoints (colour-coded groups) in terms of the resulting CD8β signal strength. The pseudo-colour plots represent the lymphocytes of a single representative animal (A). The experiment was performed with samples from five different animals. In the boxplots the frequencies of $CD8\beta^+$ lymphocytes (B) and the MFI of CD8β (C) are shown. Individual tested animals are represented by different symbols (circle, square, triangle, diamond, asterisk). The middle line of each boxplot indicates the median of the tested animals for every group.

In the fourth experiment, the interactions between the anti-CD8α 11/295/33 mAb clone, labelled with Alexa-488 and another anti-CD8β mAb clone (PG164A), labelled with Alexa-647 were investigated. Here we had to use directly labelled antibodies as both clones were of the same isotype. In the pseudo-colour plots, a strong decrease in the CD8β signal could be seen at each stage compared to the control group (w/o, %: 14.3 / MFI: 6974). The decrease was strongest when the 11/295/33 and the PG164A clones were added at the same time (%: 0.39 / MFI: 840) and when the 11/295/33 clone was added before the PG164A clone (%: 1.18 / MFI: 992). Adding the 11/295/33 clone delayed by five minutes after the PG164A clone led to a greater decrease in PG164A binding success (%: 1.84 / MFI: 915), than adding the 11/295/33 clone 20 minutes after the PG164A clone (%: 5.58 / MFI: 1168) (Figure 11A). The data displayed in the box plots, displaying the frequencies of $CD8\beta^+$ lymphocytes follow that of the pseudo-colour plots, in which, on average, the simultaneous addition of the 11/295/33 clone and the PG164A clone as well as the previous addition of the 11/295/33 clone before the PG164A clone, showed the smallest $CD8\beta^+$ percentage values. The addition of the 11/295/33 clone 20 minutes after the PG164A clone led to higher $CD8\beta^+$ percentage values, than the delayed addition of the 11/295/33 clone only five minutes after adding the PG164A clone (Figure 11B). Regarding the MFI box plots of CD8β, similar effects were observed. No significant differences could be observed, and the values of every animal tested were almost identical (Figure 11C).

The fifth and final experiment of this type involved studying the interactions between the anti-CD8α 76-2-11 mAb clone, directly labelled with the fluorochrome PE and the anti-CD8β PG164A mAb clone labelled with Alexa-647. In this setup again CD8 labelling had to be performed direct, as both mAbs were of the same isotype. When looking at the pseudo-colour plots, it was noticeable that there was no clear difference between the $CD8\beta^+$ population of the control group and the $CD8\beta^+$ populations of the different groups. The pseudo-colour plots look very similar and there was no significant decrease in the CD8β signal (Figure 12A). Regarding the percentage of $CD8\beta^+$ lymphocytes (w/o %: 18), the behavior of the different animals tested did not appear to be different. The animals all had very similar values in terms of $CD8\beta^+$ lymphocyte frequencies (%: 16.5-18) (Figure 12B). In the box plots that display the MFI of CD8β, interestingly it was noticeable, that the control group had on average lower values (w/o, MFI: 19128), than the group in which the 76-2-11 clone was added about 20 minutes before the PG164A clone (MFI: 30286). The addition of the 76-2-11 clone before the PG164A clone, led

to the highest MFI values in every animal tested, compared to all other groups (MFI: 19128-30286) (Figure 12C). This phenomenon could not be observed from the pseudo-colour plots and the box plots that display the frequencies of CD8β$^+$ lymphocytes.

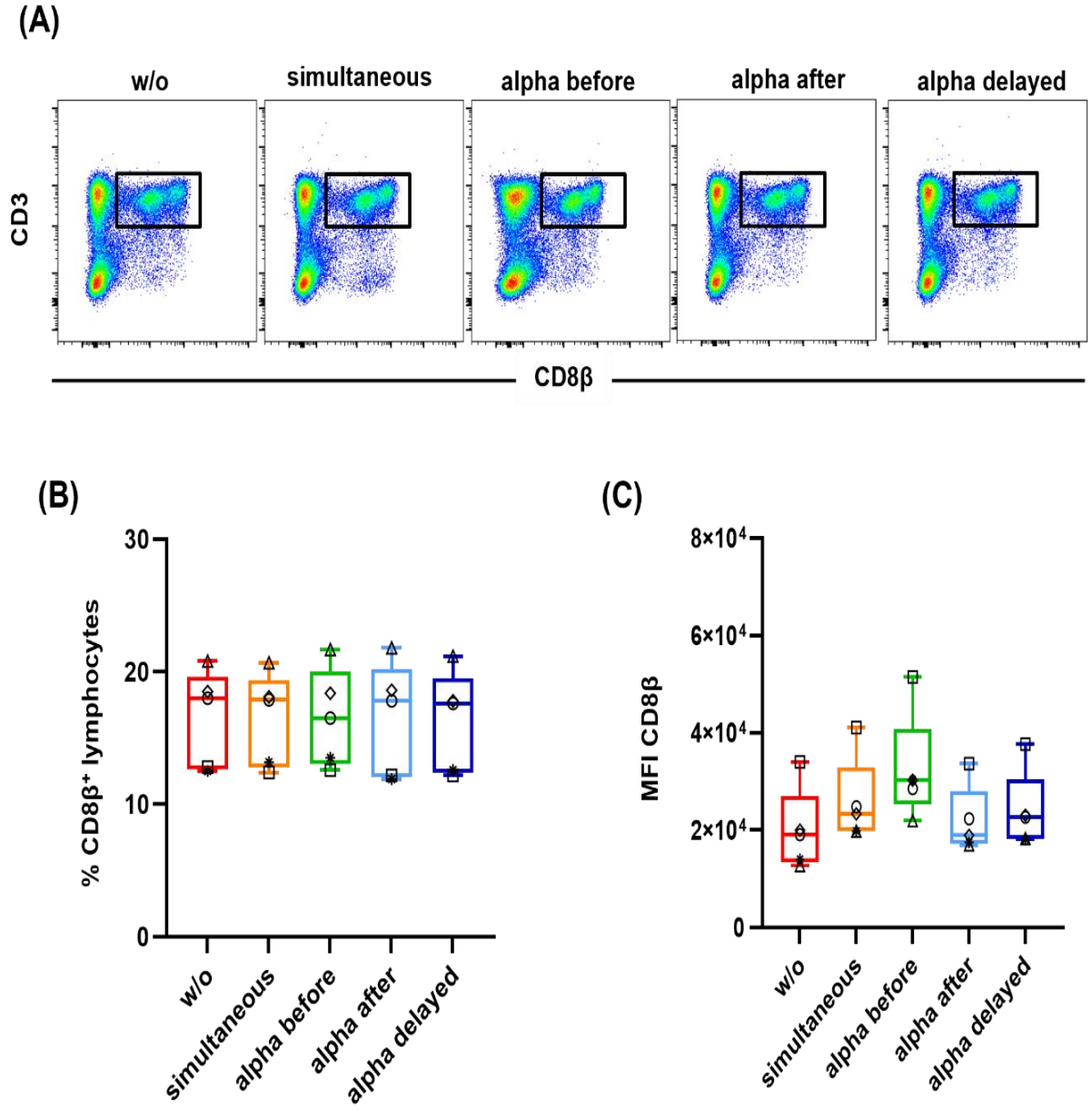

Figure 12: The effects of the 76-2-11 clone on the PG164A clone
The figure shows the effects of adding the anti-CD8α 76-2-11 mAb clone to the anti-CD8β PG164A mAb clone at different timepoints (colour-coded groups) in terms of the resulting CD8β signal strength. The pseudo-colour plots represent the lymphocytes of a single representative animal (A). The experiment was performed with samples from five different animals. In the boxplots the frequencies of CD8β$^+$ lymphocytes (B) and the MFI of CD8β (C) are shown. Individual tested animals are represented by different symbols (circle, square, triangle, diamond, asterisk). The middle line of each boxplot indicates the median of the tested animals for every group.

3.2 CD8α blocking experiments

As the effect on CD8β binding only occurred when the CD8α mAb clone 11/295/33 was used and not 76-2-11, we wanted to investigate whether the used CD8α-binding mAb clones (CD8α 11/295/33 and CD8α 76-2-11) bind to the same epitope. The interactions between the CD8α clones themselves and among each other were examined in blocking assays. In each experiment, the effects of 10-fold, equal (1.0-fold), 0.1-fold and 0.01-fold amounts of previously added primary CD8α binding antibody on the other CD8α binding antibody were tested. The results of the experiments carried out were summarized in the following graph and are represented as groups according to the added amount of primary CD8α binding antibody (Figure 13). The histogram overlay shows the resulting CD8α signal in relation to the maximum CD8α percentage value. The control group is marked in red, and the groups are ordered by decreasing amounts of previously added antibody. The box plots in the middle show the resulting frequencies of $CD8\alpha^+$ lymphocytes and the box plots on the right shows the values of the resulting MFIs of CD8α. The median of the tested animals for the frequencies and MFI of CD8α within the different groups is given as a comparative value.

First, the effect of the 11/295/33 clone blocking on itself was verified as positive control. For binding detection, the antibody was labeled with a secondary Alexa-647 antibody. From each figure, it could be seen that the obtained CD8α signal (w/o, %: 39.90 / MFI: 8614) became stronger with decreasing amount of added primary unlabeled antibody (%: 30.75-41.65 / MFI: 2182-10111). Therefore, confirming that the 11/295/33 clone had a blocking effect on itself (Figure 13A).

Subsequently, the relationship between the 295/33-25 and the 11/295/33 clone was investigated. The first mentioned was reported to be a subclone of 11/295/33, thus should also lead to similar results as described above. The 295/33-25 clone served as blocking antibody and the 11/295/33 clone, labeled with Alexa-647, was detected. It could be seen that the signal strength of CD8α (w/o, %: 39.90 / MFI: 8614) overall increased with decreasing concentration of 295/33-25 antibody clone added (%: 32.30-42.8 / MFI: 2426-11168). Therefore, the 295/33-25 clone also seemed to exert a blocking effect on the 11/295/33 clone (Figure 13B).

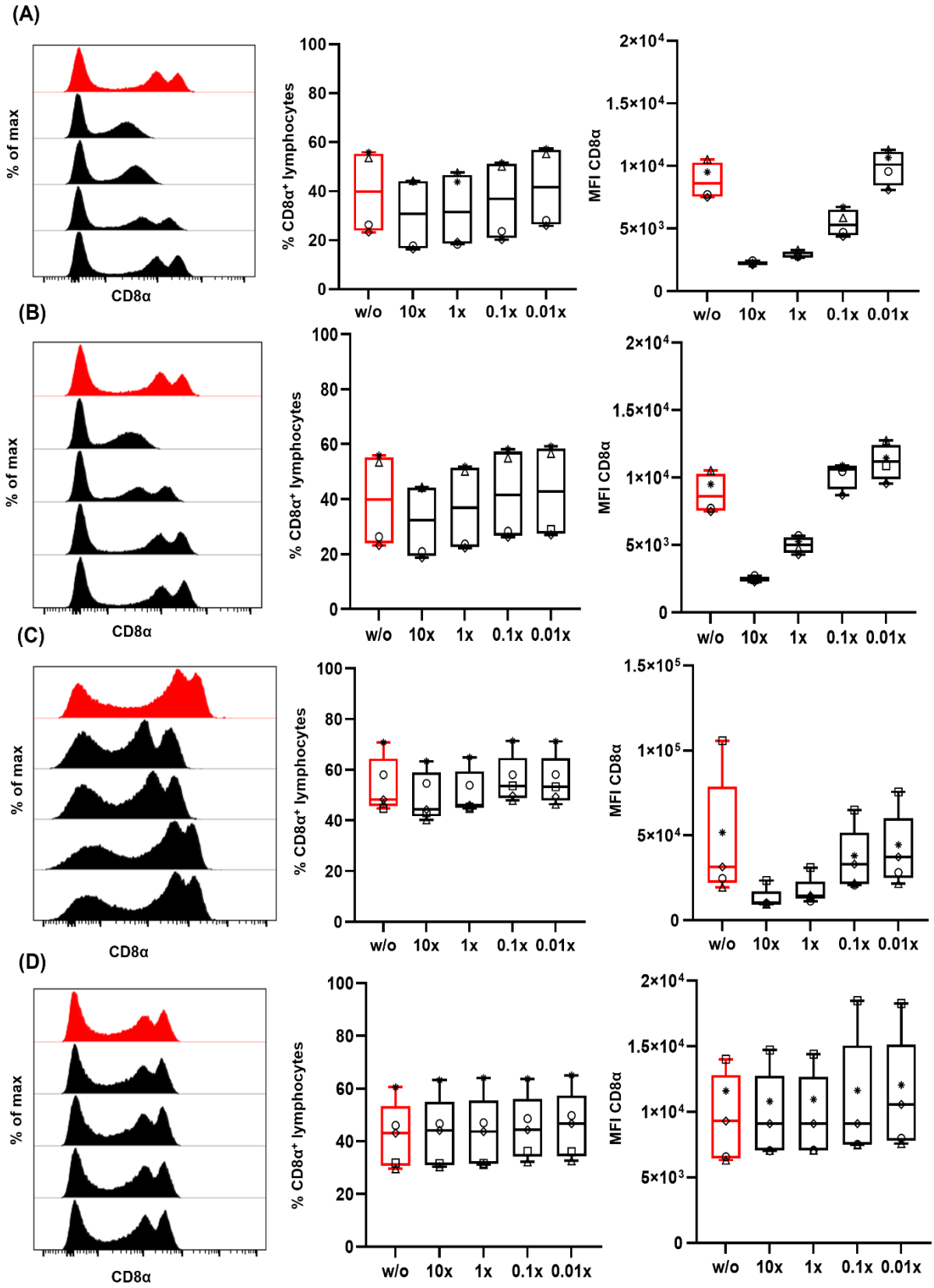

Figure 13: The influence of the CD8α clones (11/295/33, 76-2-11 and 295/33-25) between themselves and among each other

The figure shows the effects of different amounts of previously added CD8α antibody clones in the context of blocking assays. The effects of 11/295/33 on itself (A), the interactions between 295/33-25 and 11/295/33 (B), the effects of 76-2-11 on itself (C) and the interactions between 76-2-11 and 11/295/33 (D). Experiments were performed with samples from at least four different animals. The histogram overlay represents the lymphocytes of a single representative animal. The boxplots show the frequencies of $CD8\alpha^+$ lymphocytes and the MFI of CD8α. The values of the individual tested animals are represented by different symbols (circle, square, triangle, diamond, asterisk). The middle line of each boxplot indicates the median of the tested animals for every group.

Next, the impact of the 76-2-11 clone on itself was studied as part of the positive control. For binding detection, the antibody was labeled with PE by the use of a secondary antibody. The histogram overlay indicated a slight blocking effect of the 76-2-11 clone on itself. The overall frequencies of $CD8\alpha^+$ lymphocytes did not change much in every stage (%: 44.30-53.60), compared to the control group (w/o, %: 48.20 / MFI: 31445) in each animal tested. However, looking at the MFI of CD8α, the blocking effect was visible, and the overall signal became stronger with decreasing amount of previously added 76-2-11 antibody (MFI: 9886-37372) (Figure 13C).

Finally, the influence of the 76-2-11 clone on the 11/295/33 clone, labeled with Alexa-647 was analyzed. It could be observed that the amount of the 76-2-11 clone used as blocking reagent had no significant effect on the resulting CD8α signal strength measured by the 11/295/33 clone. Therefore, the 76-2-11 clone did not show an explicit inhibiting activity on the 11/295/33 clone, since the CD8α signal (w/o, %: 43.10 / MFI: 9285) did not change much with decreasing concentration of 76-2-11 clone (%: 43.10-46.70 / MFI: 9092-10556) (Figure 13D). Regarding the MFI of CD8α, in one of the animals tested (represented by the square), two outliers can be seen in the last two groups.

3.3 CD8β blocking experiments

This blocking experiments were also performed with the two different mAb clones for CD8β (PPT23 and PG164A). The binding/blocking effects of the antibodies on themselves and on the other clone for CD8β was examined as before in 10-fold, equal (1.0-fold), 0.1-fold and 0.001 fold amounts of previously added CD8β-binding antibody. The presentation of the results is identical to the previous experiments, except that they are now CD8β associated FCM signals. The median of the tested animals for the frequencies and MFI of CD8β within the different groups is given as a comparative value.

The first test involved observing the effect of the PG164A clone on itself. For signal recognition, the PG164A clone was labeled with Alexa-647. In the context of this positive control, it could be seen, that the CD8β signal strength did not really change unambiguously (w/o, %: 16.6 / MFI: 3358). A possible blocking effect of PG164A on itself, could best be supposed in the box plots regarding the MFI of CD8β. The MFI of CD8β increased slightly as the amount of previously added PG164A antibody decreased (MFI: 2176-3358) (Figure 14A).

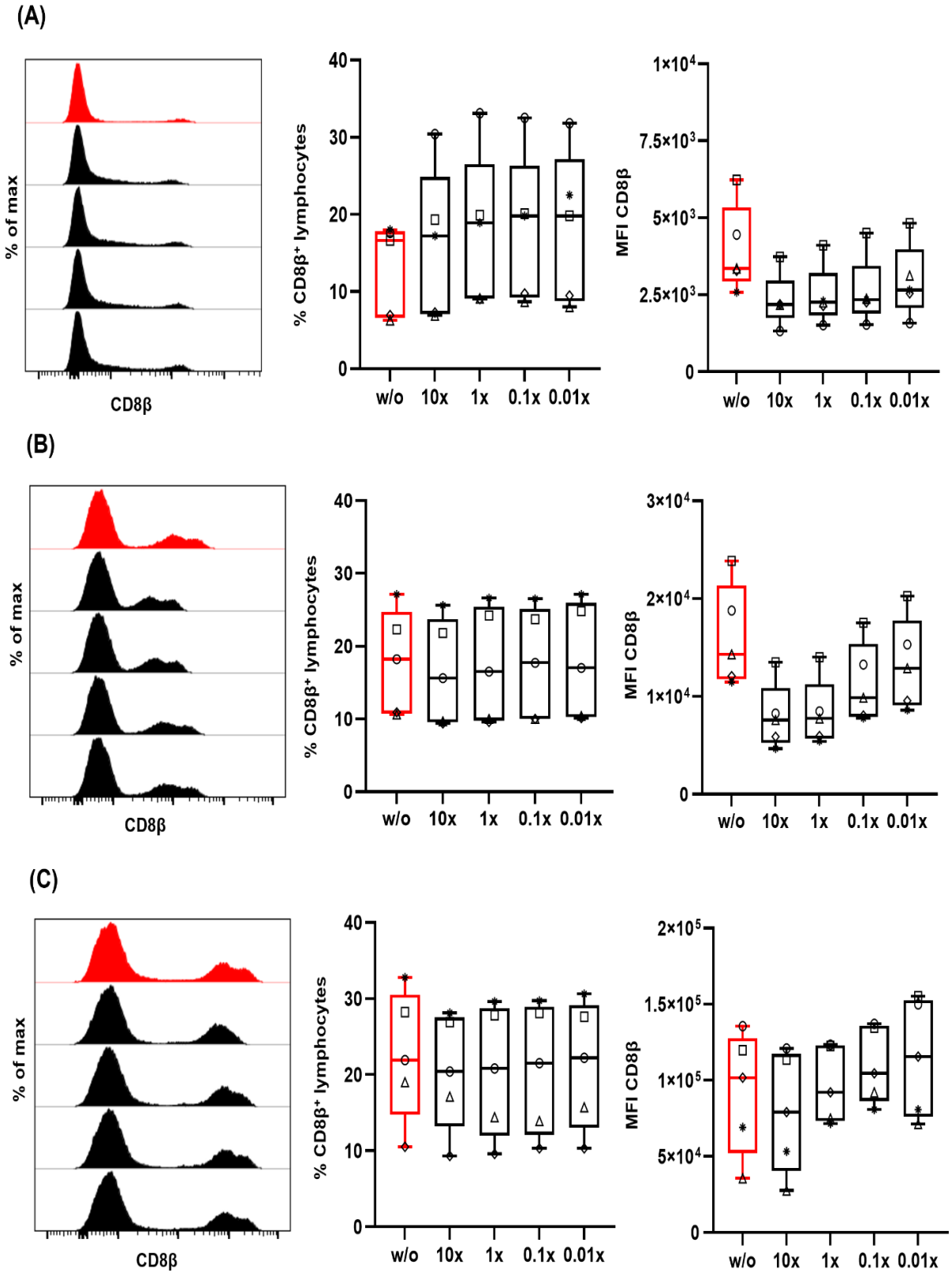

Figure 14: The influence of the CD8β clones (PPT23 and PG164A) between themselves and among each other

The figure shows the effects of different amounts of previously added CD8β antibody clones in the context of blocking assays. The effects of PG164A on itself (A), the effects of PPT23 on itself (B) and the interactions between PG164A and PPT23 (C). Experiments were performed with samples from five different animals. The histogram overlays represent the lymphocytes of a single representative animal. The boxplots show the frequencies of $CD8\beta^+$ lymphocytes and the MFI of CD8β.The values of the individual tested animals are represented by different symbols (circle, square, triangle, diamond, asterisk). The middle line of each boxplot indicates the median of the tested animals for every group.

Subsequently, the interaction of the PPT23 clone on itself was investigated as second positive control. For signal recognition, the PPT23 clone was labeled with Alexa-488. A blocking effect (w/o, %: 18.2 / MFI: 14300) was best observed with respect to the MFI of CD8β (MFI: 7581-14300). The histogram overlay and the box plots regarding the frequencies of $CD8\beta^+$ lymphocytes showed no obvious change in the values of the groups (%: 1.,6-18.2). A possible blocking effect of the PPT23 clone on itself, can therefore only be derived from the MFI box plots (Figure 14B).

Finally, the influence of the PG164A on the PPT23 clone was analyzed. For signal detection, a secondary anti-IgG1 antibody, labelled with A-488 was used. In this experiment, a clear blocking effect (w/o, %: 21.9 / MFI: 101735) of the PG164A clone on the PPT23 clone could not be reported. The MFI values of the animals tested, interestingly were not equal as between the different groups as expected (MFI: 79079-115624). The histogram overlay and the $CD8\beta^+$ lymphocyte frequencies indicated no inhibitory effect of the PG164A clone on the PPT23 clone. The frequencies of $CD8\beta^+$ lymphocytes behaved very much the same in every group and did not heavily change with the amount of previously added PG164A antibody (%: 20.4-22.2) (Figure 14C).

4 Discussion

4.1 Summary of results

Preliminary results indicate that distinct combinations of mAb clones for porcine CD8α and CD8β chains can cause troubles in multi-colour staining panels, possibly due to steric inhibition of the mAbs binding to spatial closely located epitopes. This can lead to suboptimal detection of $CD8\beta^+$ cytolytic T cells. Therefore, aim of this project was the in-depth study of the usage of different mAb clones and optimizing co-staining strategies.

To interpretate the test results, it is useful to summarize the most important findings. In the context of this thesis, experiments were performed with different mAb clones for CD8α chain detection (11/295/33, 76-2-11 and 295/33-25) and CD8β chain detection (PPT23 and PG164A). The work involved investigating the interactions of the different antibody clones with each other in FCM staining panels. For this purpose, CD8α and CD8β binding mAbs were added to porcine PBMCs at different time-points. The influence of the addition of CD8α binding antibodies on CD8β binding antibodies was then measured by the resulting CD8β FCM signal. In case of interference of the different mAbs, it could be assumed, that certain CD8α mAb clones can reduce the binding success of CD8β mAb clones, and therefore decrease the FCM signal for CD8β.

It was found that the 11/295/33 CD8α clone generally had an inhibitory effect on the two CD8β clones PPT23 and PG164A. The strongest blocking effect occured with the pre-addition of the 11/295/33 clone approximately 20 minutes before the tested CD8β clones. The simultaneous addition of 11/295/33 and PPT23 or PG164A likewise led to a noticeable loss of the corresponding CD8β signal. Applying the 11/295/33 mAb clone after the CD8β clones seemed to improve the CD8β binding process to some extent, at least for the PPT23 mAb clone. This was seen for the detection of the frequencies of total $CD8\beta^+$ cells, although still a reducing effect on the MFI of the CD8β signal was observed. However, whether 11/295/33 was added 20 minutes or just five minutes later does not appear to make any major difference in terms of blocking the PPT23 clone. Regarding the PG164A clone, the addition of 11/295/33 delayed by five minutes led to a higher blocking effect of 11/295/33 on PG164A, than the addition 20 minutes after PG164A. In contrast to this, blocking effects of the 76-2-11 clone on the two investigated CD8β mAb clones could not be reported.

As the observed blocking effect was only seen with one of the two anti-CD8α mAbs, we assumed that the 11/295/33 and the 76-2-11 clones bind different epitopes. This was confirmed as the two clones did not affect each other in their antigen binding and their corresponding FCM signal when used in blocking experiments with each other. In contrast to this, the positive control (blocking the distinct mAb clone with itself in different concentrations) showed reduction of binding, that was especially seen in the MFI. The same occurs, when looking at the interactions between the 295/33-25 and the 11/295/33 clone. We therefore assume, that the two antibodies recognize the same epitopes. The same was performed for the CD8β mAb clones. Regarding the 76-2-11 and the PG164A clone, the blocking effect on itself was lesser than for the other clones, even at the 10x concentration. This might be related to a lower affinity of the PG164A and the 76-2-11 mAb clones.

4.2 Interpretation and possible causes

4.2.1 Steric hindrance in FCM

For an antibody to bind targets like cells and pathogens, it must bind to a precisely defined specific part of the antigen, the epitope. An antigen can consist of several different epitopes. The part with which an antibody binds to its matching epitope is called paratope. Depending on the molecular structure of the paratope, an antibody binds to exactly one specific epitope. The binding of an antibody to an antigen is generally referred to as antigen-antibody reaction. This reaction is reversible and represents a non-covalent interaction. The bonding is primarily based on electrostatic interactions, hydrogen bonds, van der Waals forces and hydrophobic interactions (Kapingidza et al.2020).

When multiple epitopes are in proximity, the binding of one antibody to a first epitope may spatially hinder the binding of a second antibody to a second epitope. During binding, the antibody occupies a lot of space and takes up a position, which might be unfavourable for other antibodies. The position can block nearby epitopes (epitope masking), making it impossible for the other antibodies to bind. This process is known as steric hindrance (SH) or steric inhibition (Cowan and Underwood 1988). In the case of antigen-antibody reactions, this means that antibodies that bind close to each other to their specific epitopes might interfere with each other. Thus resulting in reduced binding of one of the antibodies, or even complete blocking of the binding (Cowan and Underwood 1988; Matos 2021).

The term steric hindrance, in the view of FCM, describes the phenomenon of reduction or complete absence of detectable fluorescent signals. It is caused by interference with the binding of one antibody to its respective target antigen or epitope by another antibody, when the two reagents are used together. For that to happen, the antibodies must bind to the same molecule, or macromolecular complex (e. g. CD8 homo- or heterodimer) and to spatially close epitopes (Matos 2021; Shah et al. 2021).

Matos et al. reported problems in the context of a diagnostic procedure of chronic lymphocytic leukemia. Steric hindrance was assumed to be the cause of the unexpected decrease in FCM fluorescence signal. For required FCM staining the antibody mixture consisting of anti-kappa, anti-lambda, anti-CD19 and anti-CD20 mAbs was used. It was considered that anti-CD19 mAbs might interfere with the binding of anti-kappa and anti-lambda mAbs by SH, because no kappa and lambda chain expression was detected on the surface of B cells. It was concluded that the cause of this effect must be due to the spatial proximity between the CD19 protein and the transmembrane immunoglobulin of the B cell receptor (Matos 2021).

In our performed experiments, the observed blocking effect of 11/295/33 on the investigated CD8β binding mAb clones, is also believed to be caused by the local proximity of the antigen binding sites on the CD8α and CD8β chains. As a result, we think that this was the main cause for the CD8β signal loss in FCM. Binding of the 11/295/33 clone to its specific epitope on the CD8α chain, probably obscures nearby epitopes on the CD8β chain and therefore make binding for the PPT23 and the PG164A clone difficult. Regarding the 76-2-11 clone, no inhibitory effect on both CD8β mAb clones could be reported. As the 76-2-11 clone probably binds to another epitope on the CD8α chain (showed by blocking experiments), we assumed that it must be located farther away from the investigated epitopes on the CD8β chain and the epitope for the 11/295/33 clone. This was also explored in a similar FCM blocking-based analyses in 1994 by A. Saalmüller et al. In the experiment, six different mAb clones for CD8 were used, including 11/295/33 and 76-2-11. Two different epitopes were detected, with 76-2-11 binding to epitope CD8a and 11/295/33 binding to epitope CD8b – both on the CD8α chain. The exact location of the two epitopes could not be determined (Saalmüller et al. 1994). Although not leading to a distinct identification of the epitopes recognized by the single mAb clones, these blocking experiments are useful to get a first idea of the same epitopes are used and performed frequently

in FCM for this purpose (Stein et al. 1993; Mair et al. 2012). Under these conditions, the two different epitopes for the PPT23 and the PG164A clone on the CD8β chain would have to be located very close to each other, since blocking of the 11/295/33 clone on both CD8β binding mAb clones was demonstrated.

The strength of a single binding interaction between antigen and antibody is described by the affinity. High affinity is equivalent to a high binding strength. Antibodies with a higher affinity to their epitopes are more difficult to prevent from binding, than those with a low affinity (Kapingidza et al. 2020). Accordingly, a high affinity leads to a stronger and more stable labelling in FCM. If the affinity is rather low, which we assume to be the case for the 76-2-11 and the PG164A clone, the bond is very unstable and is more easily be broken by several factors within the staining process. This might include the unintentional removal of antibodies by the washing process or the unsolicited displacement of an antibody by another due to a rather unstable binding. These processes could be the cause for the observed results of the positive control for the 76-2-11 and the PG164A clones. We assume that the described phenomena were also the cause for the generally increased MFI values of CD8β when the clones 76-2-11 and PG164A were added simultaneously in experiment 5 (Figure 12C).

4.2.2 Further investigations

To understand the exact mechanism of SH in the context of FCM, knowledge about the distribution of the molecules on the observed cell surface and the exact localization of the epitopes are very important requirements. Steric hindrance is often described as an asymmetric phenomenon, meaning that a certain reagent can block the binding of another, but not vice versa (Matos 2021).The underlying factors that eventually lead to blockade between antibodies are not clear and often vary widely. For example, the molecular weight of the competing fluorochromes (the combination of heavier molecules such as PE and PE-Cy5) was considered to be the causative factor for the occurrence of SH in the previously described leukemia diagnostic procedure (Matos 2021; De Vita et al. 2015). The same could account when using indirect staining strategies (primary and secondary antibody). To rule out this possibility, the experiment with the 11/295/33 and PPT23 mAb clones was repeated with directly stained mAbs, leading to the same result and thus confirming that the blocking might be rather caused

by SH. It is even possible that the degree of membrane protrusions (e. g. microvilli) on the cell surface could contribute to preventing the binding of the reagent involved (Wang et al. 2014).

In this sense, other techniques could be helpful to uncover the mechanism responsible for the occurrence of SH. Scanning electron microscopy can reveal the presence of artifacts on the surface of cells that exhibit SH. In addition to this, atomic force microscopy can be helpful for elucidating the molecular antigen-antibody mechanisms since the technique enables the determination of the adhesion force between antigen and antibody as a parameter to be measured (Matos 2021). In our approach, the final proof on distinct epitopes recognized by the mAb clones would be helpful for data interpretation. To localize the observed epitopes and obtain their specific amino acid sequence, immunological detection methods such as Enzyme Linked Immunosorbent Assays by using peptides spanning the whole molecule of interest could be valuable (Abbott et al. 2014). This approach will be the next step for the work on porcine CD8α/β and is currently in progress. Obtained information will provide a better understanding of the molecular structure (e.g., linear or conformational) and location of the epitopes and may help to further understand the mechanisms involved in SH.

Several approaches were proposed to minimize the effects of steric hindrance, if possible. First, any mAb combination used in the FCM process should be tested beforehand in comparison to single staining panels. The problem of SH can be the use of too high concentrations of the primary antibody. To determine the correct amount of antibodies to be used in the FCM process, it is recommended to perform an antibody titration. Subsequently, the problem of SH could be solved by using the correct dilution and long incubation times with the primary material. However, unexpected antibody behavior may occur even when the staining procedure is part of an already validated protocol (De Vita et al. 2015; Tangri et al. 2013; Shah et al. 2021). Or as we propose: to use another mAb clone if available.

4.3 Conclusion

In conclusion, the anti-CD8α 11/295/33 mAb clone and the anti-CD8α 295/33-25 mAb clone should not be used simultaneously with the anti-CD8β PPT23 mAb clone or the anti-CD8β PG164A mAb clone in an FCM staining panel. The 11/295/33 and the 295/33-25 clones are assumed to be subclones and therefore bind to the same epitope. The simultaneous use of these CD8α binding mAb clones, together with the observed mAb clones for CD8β, led to a reduction

of the detectable FCM signal for CD8β and thus to easily misinterpretable results as the detection of cytolytic T cells is affected. We assume that the binding of the 11/295/33 or the 295/33-25 clone to the CD8α chain complicates the binding of the PPT23 and the PG164A clone by a form of steric hindrance. Regarding the anti-CD8α 76-2-11 mAb clone, no blocking effect on the CD8β binding mAb clones could be reported. Therefore, it can be assumed that the 76-2-11 clone binds to a different spatially more distant epitope. Making the mAb combination 76-2-11 for detection of CD8α the preferable choice when planning multi-colour staining panels including both markers. This can be applied for future studies addressing CTLs (defined by the CD8β phenotype) in combination with lymphocyte subsets expressing the CD8αα homodimers (like NK cells, γδ T cells, or $CD4^+$ antigen-experienced T cells).

5 Summary

The CD8 molecule is a cell surface receptor and well described as co-receptor on T cells binding directly to the major histocompatibility complex class I on antigen presenting cells. CD8 antigens are comprised of two distinct polypeptide chains, the α and the β chain. In the pig, the CD8 receptor is expressed by several lymphocyte subsets, including Natural Killer cells, γδ T cells and antigen experienced $CD4^+$ αβ T cells. On these cell populations CD8 is expressed as αα homodimer. Porcine cytolytic T cells on the other hand exclusively express CD8 αβ heterodimers. Several monoclonal antibodies (mAbs) for either of the two chains are available and are frequently used in flow cytometry. Previous results indicate that distinct combinations of mAb clones for CD8α and CD8β chains can cause troubles in multi-colour staining panels, possibly due to steric inhibition of the antibodies binding to spacial closely located epitopes. Therefore, aim of this project was the in-depth study of the usage of different CD8-specific mAb clones and optimizing co-staining strategies. For the experiments, peripheral blood mononuclear cells were isolated by gradient centrifugation from blood of healthy pigs obtained from a conventional slaughterhouse in Lower Austria. For flow cytometric analysis mAb clones 11/295/33 and 76-2-11 were used for the detection of CD8α and clones PPT23 and PG164A for the detection of CD8β. The results indicate that the CD8α clone 11/295/33 should not be used together with either of the two CD8β clones. It can be assumed, that the antibodies bind to spatially close epitopes on the CD8α and the CD8β chains. As a result, steric hindrance occurs, leading to a highly reduced ability of CD8β mAbs in binding their specific epitopes and loss in signal in flow cytometry. In case of the CD8α mAb clone 76-2-11, no inhibition of CD8β binding was observed. Therefore, we assumed that CD8α mAb clones 11/295/33 and 76-2-11 bind to different epitopes on the CD8α chain, that are distant from each other. This was confirmed in blocking experiments using both CD8α-specific mAb clones in combination where no effects on the staining intensities were observed. The obtained data will help in future panel designs for multi-colour flow cytometry in the pig and therefore improving studies of porcine immune cells.

6 Zusammenfassung

Das CD8-Molekül ist ein Zelloberflächenrezeptor und in der Literatur als Korezeptor auf T Zellen beschrieben, der direkt an den Haupthistokompatibilitätskomplex Klasse I auf antigenpräsentierenden Zellen bindet. Für das CD8 Protein ist eine α- und eine β-Kette beschrieben. Beim Schwein wird der CD8-Rezeptor von mehreren Lymphozyten Populationen exprimiert, darunter Natürliche Killerzellen, γδ T-Zellen und Effektor/Gedächtnis $CD4^+$ αβ T Zellen. Auf diesen Zellpopulationen wird CD8 als αα-Homodimer exprimiert. Zytolytische T Zellen vom Schwein hingegen exprimieren ausschließlich CD8 αβ-Heterodimere. Mehrere monoklonale Antikörper für beide Ketten sind verfügbar und werden häufig in der Durchflusszytometrie verwendet. Frühere Ergebnisse deuten darauf hin, dass unterschiedliche Kombinationen von Antikörperklonen für CD8α- und CD8β-Ketten zu Problemen bei mehrfarbigen Panels bei der Markierung von Zellen führen können. Dies ist möglicherweise auf eine sterische Hemmung bei der Bindung der Antikörper an räumlich nahe gelegene Epitope zurückzuführen. Ziel dieses Projekts war daher die eingehende Untersuchung der Verwendung verschiedener CD8-spezifischer monoklonaler Antikörperklone in Kombination und die Optimierung von Färbungsstrategien für die Durchflusszytometrie. Für die Experimente wurden periphere mononukleäre Blutzellen durch Gradientenzentrifugation aus dem Blut von gesunden Schweinen isoliert, die aus einem konventionellen Schlachthof in Niederösterreich stammten. Für die durchflusszytometrischen Analysen wurden die monoklonalen Antikörperklone 11/295/33 und 76 2-11 für den Nachweis von CD8α und die Klone PPT23 und PG164A für den Nachweis von CD8β verwendet. Die Ergebnisse zeigten, dass der CD8α-Klon 11/295/33 nicht zusammen mit einem der beiden CD8β-Klone verwendet werden sollte. Es kann davon ausgegangen werden, dass die Antikörper an räumlich nahe beieinander liegende Epitope auf den CD8α- und CD8β-Ketten binden. Infolgedessen kommt es zu einer sterischen Behinderung, was zu einer stark reduzierten Fähigkeit der CD8β-bindenden monoklonalen Antikörper führt, ihre spezifischen Epitope zu binden. Dementsprechend kam es zu einem Signalverlust in der Durchflusszytometrie und einer suboptimalen Detektion der zytolytischen T-Zellen. Im Falle des CD8α Klons 76-2-11 wurde keine Hemmung der CD8β-Bindung beobachtet. Daher nahmen wir an, dass die CD8α-Klone 11/295/33 und 76-2-11 an unterschiedliche Epitope auf der CD8α Kette binden. Dies wurde in Blockierungsexperimenten bestätigt, bei denen beide CD8α-spezifischen monoklonale Antikörperklone in Kombination

verwendet wurden - ohne Auswirkungen auf die Markierung. Die gewonnenen Daten werden bei der Gestaltung künftiger Panels für die Mehrfarben-Durchflusszytometrie beim Schwein hilfreich sein und somit die Untersuchung von Immunzellen beim Schwein verbessern.

7 References

Abbott, W. Mark, Melissa M. Damschroder, and David C. Lowe. 2014. 'Current Approaches to Fine Mapping of Antigen-Antibody Interactions'. *Immunology* 142 (4): 526–35. https://doi.org/10.1111/imm.12284.

Adan, Aysun, Günel Alizada, Yağmur Kiraz, Yusuf Baran, and Ayten Nalbant. 2017. 'Flow Cytometry: Basic Principles and Applications'. *Critical Reviews in Biotechnology* 37 (2): 163–76. https://doi.org/10.3109/07388551.2015.1128876.

Anderson, G., N. C. Moore, J. J. Owen, and E. J. Jenkinson. 1996. 'Cellular Interactions in Thymocyte Development'. *Annual Review of Immunology* 14: 73–99. https://doi.org/10.1146/annurev.immunol.14.1.73.

Charerntantanakul, Wasin, and James A. Roth. 2006. 'Biology of Porcine T Lymphocytes'. *Animal Health Research Reviews* 7 (1–2): 81–96. https://doi.org/10.1017/S1466252307001235.

Chi, Xiying, Yue Li, and Xiaoyan Qiu. 2020. 'V(D)J Recombination, Somatic Hypermutation and Class Switch Recombination of Immunoglobulins: Mechanism and Regulation'. *Immunology* 160 (3): 233–47. https://doi.org/10.1111/imm.13176.

Cowan, R., and P. A. Underwood. 1988. 'Steric Effects in Antibody Reactions with Polyvalent Antigen'. *Journal of Theoretical Biology* 132 (3): 319–35. https://doi.org/10.1016/s0022-5193(88)80218-2.

Dawson, Harry. 2011. 'A Comparative Assessment of the Pig, Mouse and Human Genomes: Structural and Functional Analysis of Genes Involved in Immunity and Inflammation'. In *The Minipig in Biomedical Research*, by Peter McAnulty, Anthony Dayan, Niels-Christian Ganderup, and Kenneth Hastings, 323–42. CRC Press. https://doi.org/10.1201/b11356-28.

De Vita, Martina, Valentina Catzola, Alexia Buzzonetti, Marco Fossati, Alessandra Battaglia, Loris Zamai, and Andrea Fattorossi. 2015. 'Unexpected Interference in Cell Surface Staining by Monoclonal Antibodies to Unrelated Antigens'. *Cytometry. Part B, Clinical Cytometry* 88 (5): 352–54. https://doi.org/10.1002/cyto.b.21197.

Denyer, Michael S., Thomas E. Wileman, Catrina M. A. Stirling, Bartek Zuber, and Haru-Hisa Takamatsu. 2006. 'Perforin Expression Can Define CD8 Positive Lymphocyte Subsets in Pigs Allowing Phenotypic and Functional Analysis of Natural Killer, Cytotoxic T, Natural Killer T and MHC Un-Restricted Cytotoxic T-Cells'. *Veterinary Immunology and Immunopathology* 110 (3): 279–92. https://doi.org/10.1016/j.vetimm.2005.10.005.

Devine, L., J. Sun, M. R. Barr, and P. B. Kavathas. 1999. 'Orientation of the Ig Domains of CD8 Alpha Beta Relative to MHC Class I'. *Journal of Immunology (Baltimore, Md.: 1950)* 162 (2): 846–51.

Gerdts, Volker, Heather L. Wilson, Francois Meurens, Sylvia van Drunen Littel - van den Hurk, Don Wilson, Stewart Walker, Colette Wheler, Hugh Townsend, and Andrew A. Potter. 2015. 'Large Animal Models for Vaccine Development and Testing'. *ILAR Journal* 56 (1): 53–62. https://doi.org/10.1093/ilar/ilv009.

Gerner, Wilhelm, Tobias Käser, and Armin Saalmüller. 2009. 'Porcine T Lymphocytes and NK Cells – An Update'. *Developmental & Comparative Immunology*, The Porcine Immune System, 33 (3): 310–20. https://doi.org/10.1016/j.dci.2008.06.003.

Jonjić, S., and U. H. Koszinowski. 1984. 'Monoclonal Antibodies Reactive with Swine Lymphocytes. I. Antibodies to Membrane Structures That Define the Cytolytic T Lymphocyte Subset in the Swine'. *Journal of Immunology (Baltimore, Md.: 1950)* 133 (2): 647–52.

Kapingidza, A. Brenda, Krzysztof Kowal, and Maksymilian Chruszcz. 2020. 'Antigen–Antibody Complexes'. In *Vertebrate and Invertebrate Respiratory Proteins, Lipoproteins and Other Body Fluid Proteins*, edited by Ulrich Hoeger and J. Robin Harris, 94:465–97. Subcellular Biochemistry. Cham: Springer International Publishing. https://doi.org/10.1007/978-3-030-41769-7_19.

Käser, Tobias. 2021. 'Swine as Biomedical Animal Model for T-Cell Research—Success and Potential for Transmittable and Non-Transmittable Human Diseases'. *Molecular Immunology* 135 (July): 95–115. https://doi.org/10.1016/j.molimm.2021.04.004.

Köhler, G., and C. Milstein. 1975. 'Continuous Cultures of Fused Cells Secreting Antibody of Predefined Specificity'. *Nature* 256 (5517): 495–97. https://doi.org/10.1038/256495a0.

Kumar, Himanshu, and Taro Kawai. 2011. 'Pathogen Recognition by the Innate Immune System'. *International Reviews of Immunology* 30 (1): 16–34. https://doi.org/10.3109/08830185.2010.529976.

Lagumdzic, Emil, Clara Pernold, Marta Viano, Simone Olgiati, Michael W. Schmitt, Kerstin H. Mair, and Armin Saalmüller. 2022. 'Transcriptome Profiling of Porcine Naïve, Intermediate and Terminally Differentiated CD8+ T Cells'. *Frontiers in Immunology* 13: 849922. https://doi.org/10.3389/fimmu.2022.849922.

Ma, Hui, and Richard O'Kennedy. 2015. 'The Structure of Natural and Recombinant Antibodies'. *Methods in Molecular Biology (Clifton, N.J.)* 1348: 7–11. https://doi.org/10.1007/978-1-4939-2999-3_2.

Mair, K. H., C. Sedlak, T. Käser, A. Pasternak, B. Levast, W. Gerner, A. Saalmüller, et al. 2014. 'The Porcine Innate Immune System: An Update'. *Developmental and Comparative Immunology* 45 (2): 321–43. https://doi.org/10.1016/j.dci.2014.03.022.

Mair, Kerstin H., Sabine E. Essler, Martina Patzl, Anne K. Storset, Armin Saalmüller, and Wilhelm Gerner. 2012. 'NKp46 Expression Discriminates Porcine NK Cells with Different Functional Properties'. *European Journal of Immunology* 42 (5): 1261–71. https://doi.org/10.1002/eji.201141989.

Mair, Kerstin H., Andrea Müllebner, Sabine E. Essler, J. Catharina Duvigneau, Anne K. Storset, Armin Saalmüller, and Wilhelm Gerner. 2013. 'Porcine CD8αdim/-NKp46high NK Cells Are in a Highly Activated State'. *Veterinary Research* 44 (1): 13. https://doi.org/10.1186/1297-9716-44-13.

Martins, C. L., M. J. Lawman, T. Scholl, C. A. Mebus, and J. K. Lunney. 1993. 'African Swine Fever Virus Specific Porcine Cytotoxic T Cell Activity'. *Archives of Virology* 129 (1–4): 211–25. https://doi.org/10.1007/BF01316896.

Matos, Daniel Mazza. 2021. 'Steric Hindrance: A Practical (and Frequently Forgotten) Problem in Flow Cytometry'. *Cytometry. Part B, Clinical Cytometry* 100 (4): 397–401. https://doi.org/10.1002/cyto.b.21959.

McComb, Scott, Aude Thiriot, Bassel Akache, Lakshmi Krishnan, and Felicity Stark. 2019. 'Introduction to the Immune System'. In *Immunoproteomics: Methods and Protocols*, edited by Kelly M. Fulton and Susan M. Twine, 1–24. Methods in Molecular Biology. New York, NY: Springer. https://doi.org/10.1007/978-1-4939-9597-4_1.

McKinnon, Katherine M. 2018. 'Flow Cytometry: An Overview'. *Current Protocols in Immunology* 120 (February): 5.1.1-5.1.11. https://doi.org/10.1002/cpim.40.

Moretta, A., E. Marcenaro, S. Parolini, G. Ferlazzo, and L. Moretta. 2008. 'NK Cells at the Interface between Innate and Adaptive Immunity'. *Cell Death and Differentiation* 15 (2): 226–33. https://doi.org/10.1038/sj.cdd.4402170.

Nelson, P. N., G. M. Reynolds, E. E. Waldron, E. Ward, K. Giannopoulos, and P. G. Murray. 2000. 'Monoclonal Antibodies'. *Molecular Pathology: MP* 53 (3): 111–17. https://doi.org/10.1136/mp.53.3.111.

Pabst, Reinhard. 2020. 'The Pig as a Model for Immunology Research'. *Cell and Tissue Research* 380 (2): 287–304. https://doi.org/10.1007/s00441-020-03206-9.

Pescovitz, M. D., J. K. Lunney, and D. H. Sachs. 1984. 'Preparation and Characterization of Monoclonal Antibodies Reactive with Porcine PBL'. *Journal of Immunology (Baltimore, Md.: 1950)* 133 (1): 368–75.

Posner, J., P. Barrington, T. Brier, and A. Datta-Mannan. 2019. 'Monoclonal Antibodies: Past, Present and Future'. In *Concepts and Principles of Pharmacology*, edited by James E. Barrett, Clive P. Page, and Martin C. Michel, 260:81–141. Handbook of Experimental Pharmacology. Cham: Springer International Publishing. https://doi.org/10.1007/164_2019_323.

Reutner, Katharina, Judith Leitner, Sabine E. Essler, Kirsti Witter, Martina Patzl, Peter Steinberger, Armin Saalmüller, and Wilhelm Gerner. 2012. 'Porcine CD27: Identification, Expression and Functional Aspects in Lymphocyte Subsets in Swine'. *Developmental & Comparative Immunology* 38 (2): 321–31. https://doi.org/10.1016/j.dci.2012.06.011.

Reutner, Katharina, Judith Leitner, Andrea Müllebner, Andrea Ladinig, Sabine E. Essler, J. Catharina Duvigneau, Mathias Ritzmann, Peter Steinberger, Armin Saalmüller, and Wilhelm Gerner. 2013. 'CD27 Expression Discriminates Porcine T Helper Cells with Functionally Distinct Properties'. *Veterinary Research* 44 (1): 18. https://doi.org/10.1186/1297-9716-44-18.

Saalmüller, A., B. Aasted, A. Canals, J. Dominguez, T. Goldman, J. K. Lunney, S. Maurer, M. D. Pescovitz, R. Pospisil, and H. Salmon. 1994. 'Analyses of MAb Reactive with Porcine CD8'. *Veterinary Immunology and Immunopathology* 43 (1–3): 249–54. https://doi.org/10.1016/0165-2427(94)90144-9.

Saalmüller, A., T. Pauly, B. J. Höhlich, and E. Pfaff. 1999. 'Characterization of Porcine T Lymphocytes and Their Immune Response against Viral Antigens'. *Journal of Biotechnology* 73 (2–3): 223–33. https://doi.org/10.1016/s0168-1656(99)00140-6.

Saalmüller, A., M. J. Reddehase, H. J. Bühring, S. Jonjić, and U. H. Koszinowski. 1987. 'Simultaneous Expression of CD4 and CD8 Antigens by a Substantial Proportion of Resting Porcine T Lymphocytes'. *European Journal of Immunology* 17 (9): 1297–1301. https://doi.org/10.1002/eji.1830170912.

Saalmüller, Armin. 2006. ‘New Understanding of Immunological Mechanisms’. *Veterinary Microbiology*, Canine and Feline Vaccination - A Scientific Re-appraisal, 117 (1): 32–38. https://doi.org/10.1016/j.vetmic.2006.04.007.

Saalmüller, Armin, Tobias Werner, and Vicky Fachinger. 2002. ‘T-Helper Cells from Naive to Committed’. *Veterinary Immunology and Immunopathology*, Fossum S. I., 87 (3): 137–45. https://doi.org/10.1016/S0165-2427(02)00045-4.

Sedlak, Corinna, Martina Patzl, Armin Saalmüller, and Wilhelm Gerner. 2014. ‘CD2 and CD8α Define Porcine Γδ T Cells with Distinct Cytokine Production Profiles’. *Developmental and Comparative Immunology* 45 (1): 97–106. https://doi.org/10.1016/j.dci.2014.02.008.

Shah, Kalpesh, Amr Rajab, Teri Oldaker, Andrea Illingworth, and Ann Taylor. 2021. ‘Selection and Validation Strategy for Adding Antibodies to Flow Cytometry Panels’, March. https://www.cytometry.org/web/modules/Module_21.pdf.

Shishido, Stephanie N., Sriram Varahan, Kai Yuan, Xiangdong Li, and Sherry D. Fleming. 2012. ‘Humoral Innate Immune Response and Disease’. *Clinical Immunology (Orlando, Fla.)* 144 (2): 142–58. https://doi.org/10.1016/j.clim.2012.06.002.

Sinkora, M., J. Sinkora, Z. Reháková, and J. E. Butler. 2000. ‘Early Ontogeny of Thymocytes in Pigs: Sequential Colonization of the Thymus by T Cell Progenitors’. *Journal of Immunology (Baltimore, Md.: 1950)* 165 (4): 1832–39. https://doi.org/10.4049/jimmunol.165.4.1832.

Sinkora, M., J. Sinkora, Z. Reháková, I. Splíchal, H. Yang, R. M. Parkhouse, and I. Trebichavsk. 1998. ‘Prenatal Ontogeny of Lymphocyte Subpopulations in Pigs’. *Immunology* 95 (4): 595–603. https://doi.org/10.1046/j.1365-2567.1998.00641.x.

Sinkora, Marek, and John E. Butler. 2009. ‘The Ontogeny of the Porcine Immune System’. *Developmental and Comparative Immunology* 33 (3): 273–83. https://doi.org/10.1016/j.dci.2008.07.011.

Stein, R., E. Belisle, H. J. Hansen, and D. M. Goldenberg. 1993. ‘Epitope Specificity of the Anti-(B Cell Lymphoma) Monoclonal Antibody, LL2’. *Cancer Immunology, Immunotherapy: CII* 37 (5): 293–98. https://doi.org/10.1007/BF01518451.

Takamatsu, H.-H., M. S. Denyer, C. Stirling, S. Cox, N. Aggarwal, P. Dash, T. E. Wileman, and P. V. Barnett. 2006. ‘Porcine Gammadelta T Cells: Possible Roles on the Innate and Adaptive Immune Responses Following Virus Infection’. *Veterinary Immunology and Immunopathology* 112 (1–2): 49–61. https://doi.org/10.1016/j.vetimm.2006.03.011.

Talker, Stephanie C., Tobias Käser, Katharina Reutner, Corinna Sedlak, Kerstin H. Mair, Hanna Koinig, Robert Graage, et al. 2013. ‘Phenotypic Maturation of Porcine NK- and T-Cell Subsets’. *Developmental & Comparative Immunology* 40 (1): 51–68. https://doi.org/10.1016/j.dci.2013.01.003.

Talker, Stephanie C., Hanna C. Koinig, Maria Stadler, Robert Graage, Eva Klingler, Andrea Ladinig, Kerstin H. Mair, et al. 2015. ‘Magnitude and Kinetics of Multifunctional CD4+ and CD8β+ T Cells in Pigs Infected with Swine Influenza A Virus’. *Veterinary Research* 46 (1): 52. https://doi.org/10.1186/s13567-015-0182-3.

Tangri, Shabnam, Horacio Vall, David Kaplan, Bob Hoffman, Norman Purvis, Anna Porwit, Ben Hunsberger, T. Vincent Shankey, and ICSH/ICCS Working Group. 2013. ‘Validation of Cell-Based

Fluorescence Assays: Practice Guidelines from the ICSH and ICCS - Part III - Analytical Issues'. *Cytometry. Part B, Clinical Cytometry* 84 (5): 291–308. https://doi.org/10.1002/cyto.b.21106.

Terry, L. A., J. P. DiSanto, T. N. Small, and N. Flomenberg. 1990. 'Differential Expression and Regulation of the Human CD8 Alpha and CD8 Beta Chains'. *Tissue Antigens* 35 (2): 82–91. https://doi.org/10.1111/j.1399-0039.1990.tb01761.x.

Thome, M., W. Hirt, E. Pfaff, M. J. Reddehase, and A. Saalmüller. 1994. 'Porcine T-Cell Receptors: Molecular and Biochemical Characterization'. *Veterinary Immunology and Immunopathology* 43 (1–3): 13–18. https://doi.org/10.1016/0165-2427(94)90115-5.

Wang, Meiyao, Martin Misakian, Hua-Jun He, Peter Bajcsy, Fatima Abbasi, Jeffrey M. Davis, Kenneth D. Cole, Illarion V. Turko, and Lili Wang. 2014. 'Quantifying CD4 Receptor Protein in Two Human CD4+ Lymphocyte Preparations for Quantitative Flow Cytometry'. *Clinical Proteomics* 11 (1): 43. https://doi.org/10.1186/1559-0275-11-43.

Yang, H., and R. M. Parkhouse. 1996. 'Phenotypic Classification of Porcine Lymphocyte Subpopulations in Blood and Lymphoid Tissues'. *Immunology* 89 (1): 76–83. https://doi.org/10.1046/j.1365-2567.1996.d01-705.x.

Yang, H., and R. M. Parkhouse.1997. 'Differential Expression of CD8 Epitopes amongst Porcine CD8-Positive Functional Lymphocyte Subsets'. *Immunology* 92 (1): 45–52. https://doi.org/10.1046/j.1365-2567.1997.00308.x.

8 List of figures and tables